New Induction Applications: Volume 1

Mutual and Reflected couplings:
Mutual Inductance and Linear Wire models
Retarded Time and Spherical EM Radiation modeling
Inductive Reflections from parasitic elements and conductive planes

Robert J Distinti
www.Distinti.com
Home of New Electromagnetism

Revised for New Electromagnetism V3

The original version can be found at www.distinti.com/docs/v2

Note to Reader: The V3 models were available in 1998. I did not get around to revising this paper for V3 models until the time of my graduate thesis (2007). The derivations in the paper are sound (TBOMK); however, other info such as internet links or addresses may no longer be valid.
--R Distinti -- July 2019

Copyright Page

This book is condensed from an original work of Robert J. Distinti which was submitted to the United States Patent Office for intellectual property protection purposes. This technology and other technology developed by Robert J. Distinti are protected by a number of schemes to include issued and pending patents, trade secrets, trademarks, and copyrights.

Published by:
AREA-46 Publishing (www.area-46.com)
46 Rutland Ave, Fairfield, CT 06825

Printed in the United States of America

Library of Congress Cataloging in Publication Data available

Table of Contents

NEW INDUCTION APPLICATIONS: VOLUME 1 1

1 PREFACE 5

1.1 PREREQUISITES 5
1.2 COLOR CODING 5
1.2.1 Heading Colors 5
1.2.2 Text Colors 6

2 INTRODUCTION 7

3 NEW INDUCTION 8

4 TERMS AND DEFINITIONS 10

4.1 NEW ELECTROMAGNETISM TERMS 10
4.2 V3 DEFINITIONS 11
4.2.1 Volts and emf, V_P and V_K 11
4.2.2 DC Mutual Inductance M_0 11
4.2.3 DC Inductance L_0 13
4.3 OTHER DEFINITIONS 13
4.3.1 Retarded Time 13
4.4 METHOD OF IMAGES (MOI) 15

5 GENERAL LINEAR WIRE SOLUTIONS 17

5.1 PARALLEL TRANSVERSE FILAMENTS 17
5.1.1 Derivation 17
5.1.2 "Algorithmification" 21
5.2 PARALLEL FILAMENTS 22
5.2.1 Derivation 22
5.2.2 "Algorithmification" 25

6 ANTENNAE MODELING 28

6.1 THE HALF WAVE DIPOLE ANTENNA 29
6.1.1 Energy received at transverse position 31
6.1.2 Energy at the longitudinal position 33
6.1.3 General Dipole Radiation pattern 36
6.1.4 Conclusion 40

7 SPHERICAL WAVE MODEL 41

8 RECTANGULAR LOOPS 42

8.1 RECTANGULAR LOOP EXAMPLE 45

9 PARASITIC LOOPS 53

10 CONDUCTIVE PLANES 58

10.1 SINGLE CONDUCTIVE PLANE 58
10.2 PARALLEL CONDUCTIVE PLANES 59

11 PCB / IC TRACE CROSS-TALK 61

11.1 SINGLE CONDUCTIVE PLANE 61
11.2 DOUBLE CONDUCTIVE PLANES 63
11.3 CONCLUSION 63

12 PCB / IC TRANSFORMERS 64

13 EMI CONSIDERATIONS 65

14 TRANSMISSION LINES 67

14.1 WIRE OVER GROUND PLANE (PCB/IC) 68
14.2 TWIN PARALLEL WIRE 70

15 EXPERIMENTAL VALIDATION 73

15.1 THE INDUCTANCE TEMPLATE 73
15.2 MEASURED COUPLINGS 77
15.2.1 Standard circuit 77
15.2.2 Simple transistor current source 78
15.2.3 Other Data 81
15.3 CALCULATED COUPLINGS 82
15.3.1 The primary to secondary (Direct) coupling 82
15.3.2 Coupling with single conductive plane 83
15.3.3 Coupling with two conductive planes 84
15.3.4 Coupling with outer parasitic loop 87
15.3.5 Trace Impedance reduction: Single Plane 89
15.3.6 Trace Impedance reduction: Double Plane 90

16 CONCLUSION 92

INDEX 93

1 Preface

It is our intent to create the most reader friendly publications possible. We decided that high quality full color publishing with as many pictures and diagrams as possible is the most appropriate course of action.

We try not to assume the capability of the reader except for those skills listed in the "prerequisite" section. There are many text books that just print an answer and demean the reader by saying that the derivation is obvious. We print full derivations to help out those who may not have a strong math background.

We also understand that our readers come from many varying backgrounds and may not be familiar with certain electrical engineering short-hands such as phasor notation. We strive to use the most common techniques wherever possible in order to carry along as many readers as possible.

We strive to enlighten the reader with the power, simplicity and versatility of the New Electromagnetic models and concepts. Some of the technology shown in this book is either impossible or impractical to derive with classical electromagnetic theory.

1.1 Prerequisites

This book is intended for applications engineers and physicists. It requires a Skill Level 3+ understanding of mathematics, physics and electricity. This is the equivalent of an associate's degree in electrical engineering plus additional background in Laplace transforms. A background in wave mechanics might be helpful but is not necessary.

1.2 Color Coding

In this text we color code both headings and text. Although we may use the same colors for headings and text, the colors mean different things.

1.2.1 Heading Colors

The following are examples of color coded headings. The color helps distinguish the heading level.

1 Introduction ← Chapter headings (Level 1)

1.1 Color Coding ← Subchapter (Level 2)

1.1.1 Heading Colors ← Subchapter (Level 3)

Example 1 ← Subchapter (Level 4) not-numbered

1.2.2 Text Colors

The primary purpose for coloring the text is to provide different voices to different reader levels or to channelize information.

- Black: Read by everyone
- Sky Blue: unused.
- Lime Green: unused.
- Green: unused.
- Magenta: unused.
- Brown: unused.
- Red: Red text MUST be understood before venturing foreword.
- Violet: unused.
- Blue: Code words (see back cover).
- Grey: unused.

Red Text contains very important points that must be understood before venturing forward.

We intend to use the same color coding throughout the New Electromagnetism publications. Other publications such as the "New Electromagnetism for the Conceptually Brilliant" series makes heavy use of the colors listed above. The Conceptually brilliant series of books are intended for people who are not classically trained; however, many classically trained people use the books as a primer for New Electromagnetism; therefore, we add blocks of text in a different color which speak to classically trained scientists and engineers.

Text color coding does not apply to section headings or text in illustrations, figures and photographs.

2 Introduction

New Induction is the New Electromagnetic model for the natural phenomenon known as electromagnetic induction (described in more detail in the next section). This publication uses New Induction to explore mutual couplings and reflected couplings. These couplings include linear wire-to-wire couplings, wire-to-wire coupling with the effects of a conductive planes, loop-to-loop coupling, loop-to-loop coupling with the effects of conductive planes, parasitic loop effects, Dipole-to-Dipole (antenna) coupling, dipole-to-dipole antenna coupling with ground effects, PCB trace impedance considerations, PCB trace cross-talk and more. Many of the applications and derivations in this book are either impossible or impractical to derive from classical electromagnetic theory.

This book is accompanied by software and other supplements available from our website (see back cover). The software includes numerical integration algorithms written in C/C+, an Excel spread sheet application(s) that calculates the inductive linkage between various wire constructs to include reflected couplings. The website support pages are updated regularly; the reader is urged to visit the pages often.

The techniques shown in this book are adaptable to a wide range of technological innovation to include:

1) Printed circuit board trace cross talk calculations
2) Antennae radiation modeling (more accurate than classical methods)
3) Longitudinal and Spherical waves
4) Non-ferrous metal detectors
5) Position sensing and telemetry
6) Inductive reflectometry
7) Various sensors technologies
8) Communications technology
9) Instrumentation
10) Electromagnetic material identification
11) Noise reduction
12) Power generation and transformation

This publication is a continuation of the original New Induction paper (ni.pdf).

SEE the back cover regarding the software and other supplements that accompany this text.

3 New Induction

New Induction is the New Electromagnetic model for the natural phenomenon known as electromagnetic induction. New Induction is different from classical electromagnetic theory (Faraday's Law, Maxwell's Equations) in that it is based on a spherical magnetic model and not the donut (toroidal) shaped magnetic field of classical electromagnetism.

Unlike classical electromagnetic theory, New Induction is applicable to point charges. This applicability to point charges provides for New Electromagnetic representations of inertia, matter and anti-matter. Although these topics are not covered in this text, these derivations were the reason why the New Induction model produces what is called the Inertial field.

The spherical nature of New Induction predicts the existence of both longitudinal and transverse modes of radio communication. In fact, the application of New Induction to a simple half-wave dipole antenna system predicts the correct radiation pattern; this is not the case with classical theory since classical theory does not provide for a longitudinal effect.

The versatility and simplicity of New Induction allows very simple derivations of electromagnetic reflections from parasitic loops and conductive planes. These reflections have applications from stealth technology to multidimensional position sensing, impedance modification of communication circuits and EMI noise suppression.

The New Induction has not changed from its original form in New Electromagnetism Version 1 (V1). The only difference is changes in nomenclature and the addition of a new "Wire Form" which eliminates the wire fragment notion for those who have trouble with our fragmentary notation.

Table 1 The V3 Models For New Induction

Form	The equations
Point	$\mathbf{F} = \frac{-K_M Q_S Q_T \mathbf{a}_S}{\lvert\mathbf{r}\rvert}$
Fragment	$d^2V_K = -K_M \left(\frac{di_S}{dt}\right) \frac{d\mathbf{L}_S \bullet d\mathbf{L}_T}{\lvert\mathbf{r}\rvert}$
Wire	$V_K = -K_M \int_S \int_T \left(\frac{di_S}{dt}\right) \frac{d\mathbf{L}_S \bullet d\mathbf{L}_T}{\lvert\mathbf{r}\rvert}$
Notes	$K_M = \frac{\mu}{4\pi}$

For more information about the V3 models and use of the V3 "point-to-fragment" conversion identity, see the publication ne.pdf.

Before we get to the applications, we must discuss definitions and terminology.

4 Terms and Definitions

This chapter defines terms and notation used throughout the text.

4.1 New Electromagnetism Terms

Like classical electromagnetic literature, New Electromagnetism may have many names to describe the same thing (See the following table). For example, in classical literature, an electric field may also be called a Coulomb field.

New Electromagnetic model that describes the effect	Field Responsible for carrying the effect	Classical name for the effect	Proper New Electromagnetic Terminology	Alternate New Electromagnetic Terminology
Coulomb's Model	Electric Field	Electrostatic field Coulomb field Electric field	Positional Field Positional Force(s) Positional Effect(s)	Electric Field Electric Forces Coulomb field Coulomb force(s)
New Magnetism	Magnetic field	Magnetism	Motional Field Motional Force(s) Motional Effect(s)	Magnetic field Magnetic Force(s) Magnetic Effect(s)
New Induction	Magnetic field	Electromagnetic Induction	Inertial Field Inertial Force(s) Inertial Effect(s)	Inductive field Inductive Force(s) Inductive Effect(s)

In New Electromagnetism we have introduced new names for the fields in order to better describe the source of the field. For example, Electric fields are now called Positional fields since the observed effects are related by the relative position between charges. The field generated by a magnet or a wire carrying a constant current is called a motional field since it is created by the motion (velocity) of charges. The Inertial field is created by charge acceleration (acceleration and inertia are directly related).

Some people may be confused that we treat induction and magnetism as different effects when both are carried by magnetic fields. There is really no need for confusion since the effects of a charge accelerating (induction) and the effects of charge motion (magnetism) can be modeled as separate effects due to the fact electromagnetic fields are linear. Thus, an Inertial field is a region of space disturbed by accelerating charge(s), a Motional field is a region of space disturbed by charges in motion and an Electric field is a region of space disturbed by the presence of charge. The knowledge of what actually carries

the disturbances from the source to the target does not affect the answer that we obtain. Those readers who want to go beyond New Electromagnetism can find the actual field mechanisms in the Ethereal Mechanics series.

4.2 V3 Definitions

New Electromagnetism 3 (V3) introduces new terms and definitions which are less confusion and more appropriate than the classical definitions.

4.2.1 Volts and emf, V_P and V_K

Voltage and emf are used in both classical and V1 nomenclature. The term "electro-motive-force" (emf) is confusing since it implies a "force." A "force" would suggest that emf is a vector quantity with the units of Newtons, Newtons/Coulomb or something of that nature. Instead, emf is a scalar quantity with the units of "energy-per-coulomb" or Volts. In New Electromagnetism it is demonstrated that "emf" related to magnetic fields is more precisely defined as kinetic-energy-per-coulomb or kinetic voltage. Consequently, the classical use of V is more precisely defined as potential-energy-per-coulomb or potential voltage. To reduce the confusion, the V3 models replace emf with V_K and V with V_P. V_K is kinetic-voltage and V_P is potential-voltage. Both have the units of volts (V) which is defined as energy per charge (Joules/Coulomb).

Note: in cases where no subscript is used, potential voltage is assumed.

See ne.pdf for a more complete treatment of Kinetic and potential voltages.

4.2.2 DC Mutual Inductance M_0

Mutual inductance is the ratio between the V_K (emf) developed in a target loop (secondary) due to the current change (di/dt) in a source loop (primary). This ratio is assigned the capitol letter M and is summarized by the following general expression

$$M = -\frac{V_K(\text{sec}ondary)}{di/dt(primary)}$$

Suppose a square loop of wire (see Figure 4-1) is driven by such a high frequency signal that a complete wavelength of the signal fits in the length of a side. Logically, if one were to integrate the di/dt(p) (current change as a

function of perimeter) around the loop at any given instance in time, the result would be zero. Therefore, if a pickup wire were placed near the loop (see Figure 4-1), it is doubtful that any signal would be detected.

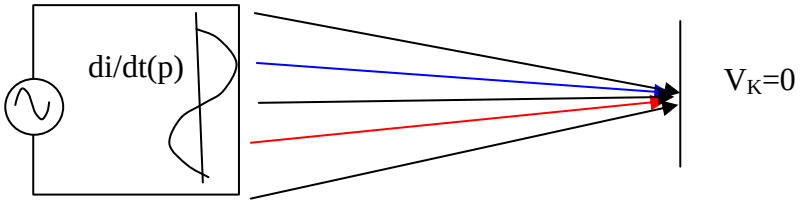

Figure 4-1

This means that the mutual inductive linkage between two wire constructs is not a constant; it varies with frequency. This may not be news to seasoned engineers and scientists; however, the realization that mutual inductance is a frequency dependant phenomenon opens doors for new types of sensors and detectors.

This variance in mutual inductance is more predominant in low-permeable core systems (such as air core transformers or antennae). Permeable core transformer data sheets show a high frequency roll-off; however, this roll-off is predominantly the result of increased core reactance and capacitive losses.

As the frequency of the signal generator in Figure 4-1 is decreased, the current change as a function of perimeter (di/dt(p)) will approach uniformity. As the frequency becomes sufficiently low, the mutual inductive linkage will not change much as a function of frequency; therefore, we introduce the "DC Mutual inductance" which is defined as the mutual inductance between two wire constructs as the signal frequency approaches zero.

$$M_0 = \lim_{di/dt \to 0} \left[\frac{V_K(\text{secondary})}{di/dt(\text{primary})} \right]$$

Equation 4-1 DC Mutual Inductive Linkage (definition)

The definition of DC inductance is important since most applications of classical and New Electromagnetism calculate M with the assumption of uniform distribution of current change in the source.

In the past, the frequency considerations of M were not of importance since it required a substantially high frequency before the value of M would be appreciably affected; however, as circuits become smaller (microscopic) and

processing signals become substantial higher, the frequency considerations of M can no longer be overlooked.

This distinction is of prime importance to this text since it contains a derivation of mutual inductive linkage between two half wave antennae using New Induction. This linkage is represented by the variable $M_{\lambda/4}$ which shows that it is an entirely different derivation from the simple DC mutual inductive linkage (also included).

Note: We are not rigorous in our usage of the subscript '0' for DC Mutual inductance. It is up to the reader to understand the type of coupling from the problem being considered.

4.2.3 DC Inductance L_0

Self induction is defined as the V_K (back emf) developed in a wire structure resulting from the current change through it. Self inductance is covered in greater detail in another related text which explores self induction, intrinsic induction and the skin-effect in great detail.

Note: We are not rigorous in our usage of the subscript '0' for DC inductance. In all instances in this book, L is the DC inductance unless specified otherwise.

4.3 Other Definitions

The terms defined in this section are retained from classical theory. We provide these definitions because they are either not found in the previous New Electromagnetism Publications or they are poorly described in classical literature.

4.3.1 Retarded Time

Retarded Time is a term used in classical electromagnetism that is horribly confusing. Retarded time seems to be something that you would build into an H.G. Wells time machine.

Retarded Time is a technique of accounting for the propagation delay of signals. Retarded Time is not directly derived from physical relationships, instead it is inferred. For example, suppose a light bulb were operated in such a way that its intensity (I) is expressed by the following relationship:

$$I = I_0\left(\frac{1}{2}\sin(2\pi ft) + \frac{1}{2}\right)$$

In the above equation, the intensity starts at ½ intensity, then continually cycles through dark and full intensity in a sinusoidal fashion. From this equation it is possible for a person to determine the instantaneous intensity (I) of the bulb at any given time (t).

But what is the instantaneous intensity observed at distance (d) from the bulb?

There are two factors that govern our ability to accurately predict the intensity at distance (d).

The first is the intensity loss as a function of distance. We know from general physics that the intensity of light diminishes proportionally to the area of a sphere; therefore, the equation is corrected by dividing through by the surface area of a sphere:

$$I = \frac{I_0}{8\pi d^2}\left(\sin(2\pi ft) + 1\right)$$

The second factor is the time it takes for a change in intensity to reach any given observer. Since we know that light travels with the finite velocity c, it takes time for a change in bulb intensity to travel to any given observer. As such, an observer at a long distance will observe a given change in intensity after an observer who is not as far.

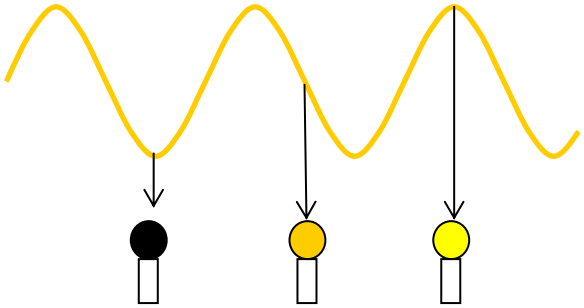

Figure 4-2 Observers at different distances see different intensities at same time

The time (T) it takes for light to reach an observer at distance d is

$$T = \frac{d}{c}$$

Since it takes time for the light to reach an observer, the light that is observed is actually light that was emitted T seconds ago by the bulb. Therefore we subtract this "Retardation factor" from the time variable in the equation to create a function that allows us to determine the intensity at any distance and at any time:

$$I(t,d) = \frac{I_0}{8\pi d^2}\left(\sin\left(2\pi f\left(t - d/c\right)\right)+1\right)$$

These retarded time techniques are used for determining light propagation and antenna radiation modeling. Antenna Radiation modeling and other applications are found in later sections of this text.

Why the term "retarded time" was chosen to name this technique is not clear.

4.4 Method of Images (MOI)

This section provides an introduction to a technique known as the "Method of Images". The "Method of Images" (MOI) is a technique used for modeling effects contributed by conductive planes. Prior to New Electromagnetism, MOI was only applicable to electrostatic systems (Coulomb's Law). The New Electromagnetic principles show that MOI has analogs in New Induction and New Magnetism as well.

The New Electromagnetism MOI covers inductive reflection and refractions for various types of materials to include conductive, ferromagnetic, paramagnetic etc.

In section 10 of this book we release a simplified form of MOI specific to induction and conductive planes. This simplified MOI is also used by amateur radio enthusiasts to characterize the effect of the ground in radio antenna theory; they call it the "Perfect Earth model." We discuss the perfect earth model in section 6.

The complete New Electromagnetism MOI, which includes complete derivations of reflections and refractions, is contained in other books in the New Electromagnetism Applications Series.

5 General Linear Wire Solutions

This section applies the New Induction model to derive exact solutions for linear wire to linear wire DC mutual inductive linkage. For the definitions of DC mutual inductive linkage see section 4.2.2.

These general solutions are included in an EXCEL spreadsheet program (NIA1.XLS) that accompanies this text.

These general solutions are applied to practical applications in later sections of this text.

Note: the parallel wire derivations that follow are not for resonant antenna applications. The resonant antenna models are derived in section 6.

5.1 Parallel Transverse Filaments

This section derives the DC mutual inductance between two parallel filamentary wires of arbitrary length and distance as shown in the following diagram.

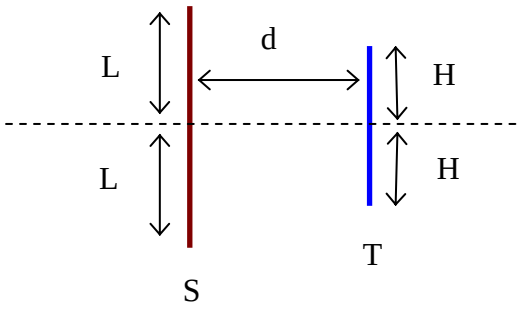

Figure 5-1 Parallel Transverse Filaments

5.1.1 Derivation

We begin the derivation by starting with the wire form of New Induction

$$1)\ V_K = -K_M \int_S \int_T \left(\frac{dI_S}{dt} \right) \frac{d\mathbf{L}_S \bullet d\mathbf{L}_T}{|\mathbf{r}|}$$

Then solve for DC mutual inductance by dividing through by the negative of the changing source current. This is done since di/dt is constant over the source and does not have to be integrated.

2) $$M_0 = K_M \int_S \int_T \frac{d\mathbf{L}_S \bullet d\mathbf{L}_T}{|\mathbf{r}|}$$

The distance (r) between source and target fragments is

3) $$r = \sqrt{(S-T)^2 + d^2}$$

Because the wires are parallel, we can drop the dot product. Also, for the sake of simplicity, we integrate the source from –L to +L and the target from –H to +H. This is done to eliminate carrying along a plethora of T/2 and S/2 terms. The equation then becomes

4) $$M_0 = K_M \int_{S=-L}^{+L} \int_{T=-H}^{+H} \frac{dSdT}{\sqrt{(S-T)^2 + d^2}}$$

We begin hammering through the integration by substituting U=(S-T). This gives dU/dT=-1 and

5) $$M_0 = -K_M \int_{S=-L}^{+L} \int_{U=(S+H)}^{(S-H)} \frac{dSdU}{\sqrt{U^2 + d^2}}$$

Using form 157 (CRC tables edition 28)

6) $$M_0 = -K_M \int_{S=-L}^{+L} \left(\ln\left(S - H + \sqrt{(S-H)^2 + d^2} \right) - \ln\left(S + H + \sqrt{(S+H)^2 + d^2} \right) \right) dS$$

Consequently

7) $$M_0 = -K_M \left[\int_{S=-L}^{+L} \ln\left(S - H + \sqrt{(S-H)^2 + d^2} \right) dS - \int_{S=-L}^{+L} \ln\left(S + H + \sqrt{(S+H)^2 + d^2} \right) dS \right]$$

Performing the left integrand first

8) $\int_{S=-L}^{+L} \ln\left(S-H+\sqrt{(S-H)^2+d^2}\right)dS$ (left side of step 7)

Substitute U=(S-H), dU/dS=1, lower limit=(-L-H) and upper limit=(L-H)

9) $\int_{U=(-L-H)}^{+L-H} \ln\left(U+\sqrt{U^2+d^2}\right)dU$

Using form 511 (CRC tables edition 28)

10) $\left[U\ln(U+\sqrt{U^2+d^2})-\sqrt{U^2+d^2}\right]_{U=-L-H}^{U=L-H}$

Substituting the limits

11) $$\begin{aligned}&(L-H)\ln\left((L-H)+\sqrt{(L-H)^2+d^2}\right)-\sqrt{(L-H)^2+d^2}\\&-(-L-H)\ln\left((-L-H)+\sqrt{(-L-H)^2+d^2}\right)+\sqrt{(-L-H)^2+d^2}\end{aligned}$$

Reducing and applying $-K_M$ from step 7 yields the first partial results

12) $$K_M\begin{bmatrix}-(L-H)\ln\left((L-H)+\sqrt{(L-H)^2+d^2}\right)+\sqrt{(L-H)^2+d^2}\\-(L+H)\ln\left(-(L+H)+\sqrt{(L+H)^2+d^2}\right)-\sqrt{(L+H)^2+d^2}\end{bmatrix}$$

We put the results in step 12 aside and complete the right side of step 7

13) $-\int_{S=-L}^{+L} \ln\left(S+H+\sqrt{(S+H)^2+d^2}\right)dS$ (right side of step 7)

Substitute U=S+H, dU/dS=1, lower limit=(-L+H) upper=(L+H)

14) $-\int_{U=-L+H}^{+L+H} \ln\left(U+\sqrt{U^2+d^2}\right)dU$

Using form 511 (CRC tables edition 28)

15) $$-\left[U\ln(U+\sqrt{U^2+d^2})-\sqrt{U^2+d^2}\right]_{U=-L-H}^{U=L-H}$$

Substituting

16) $$\begin{aligned}&-(L+H)\ln\left((L+H)+\sqrt{(L+H)^2+d^2}\right)+\sqrt{(L+H)^2+d^2}\\&+(-L+H)\ln\left((-L+H)+\sqrt{(-L+H)^2+d^2}\right)-\sqrt{(-L+H)^2+d^2}\end{aligned}$$

Reducing and applying -K_M From step 7

17) $$K_M\begin{bmatrix}+(L+H)\ln\left((L+H)+\sqrt{(L+H)^2+d^2}\right)-\sqrt{(L+H)^2+d^2}\\+(L-H)\ln\left(-(L-H)+\sqrt{(L-H)^2+d^2}\right)+\sqrt{(L-H)^2+d^2}\end{bmatrix}$$

Summing steps 17 and 12

$$M_0=K_M\begin{bmatrix}2\sqrt{(L-H)^2+d^2}-2\sqrt{(L+H)^2+d^2}\\+(L-H)\ln\left(\dfrac{-(L-H)+\sqrt{(L-H)^2+d^2}}{(L-H)+\sqrt{(L-H)^2+d^2}}\right)\\-(L+H)\ln\left(\dfrac{-(L+H)+\sqrt{(L+H)^2+d^2}}{(L+H)+\sqrt{(L+H)^2+d^2}}\right)\end{bmatrix}$$

Equation 5-1 General Solution for parallel transverse filaments

The above equation is the general solution for Parallel Transverse aligned filaments. In the above equation L=S/2 and H=T/2

A special case of the above equations is realized when the filaments are the same size (S=T). We start this derivation by setting L=H

18) $$M_0=K_M\begin{bmatrix}2d-2\sqrt{(2H)^2+d^2}\\-(2H)\ln\left(\dfrac{-2H+\sqrt{(2H)^2+d^2}}{(2H)+\sqrt{(2H)^2+d^2}}\right)\end{bmatrix}$$

Since S=T (thus L=H) we substitute H=S/2

$$M_0 = K_M \left[\begin{array}{l} 2d - 2\sqrt{S^2 + d^2} \\ -S \ln\left(\dfrac{-S + \sqrt{S^2 + d^2}}{S + \sqrt{S^2 + d^2}} \right) \end{array} \right]$$

Equation 5-2 General Solution for parallel transverse filaments of same size

5.1.2 "Algorithmification"

The first step to converting the expression in Equation 5-1 to a computer algorithm is to make the following substitutions:

$$L = S/2$$
$$H = T/2$$
$$A = L - H$$
$$B = L + H$$
$$AA = sqrt(A*A + d*d)$$
$$BB = sqrt(B*B + d*d)$$

Which yields:

$$M_0 = K_M \left[2AA - 2BB + A\ln\left(\frac{-A + AA}{A + AA} \right) - B\ln\left(\frac{-B + BB}{B + BB} \right) \right]$$

The C++ Algorithm

```
DOUBLE DC_mutual_transverse_parallel_filaments(DOUBLE S, DOUBLE T, DOUBLE d){
    DOUBLE H,L,A,B,AA,BB,DD,AAA,BBB, result;
    H=T/2;
    L=S/2;
    A=L-H;
    B=L+H;
    DD=d*d;
    AA=sqrt(A*A+DD);
    BB=sqrt(B*B+DD);
    AAA=A+AA;          // check denominators for zero
    BBB=B+BB;
    if(!(AAA && BBB))goto error;      // Test to avoid exception
    AAA=(AA-A)/AAA;
    BBB=(BB-B)/BBB;
    if(!(AAA>0 && BBB>0))goto error;  // Test to avoid exception
    result=Km*(2*(AA-BB)+A*log(AAA)-B*log(BBB));
    return result;
error:
    // Place warning here that illegal parameters detected ;
    result=-DBL_MAX;   //return near infinity ( this is arbitrary
    return result;
}
```


The Excel Algorithm

Accompanying this text is an EXCEL (NIA1.XLS) spread sheet that contains the Parallel Transverse Filament equation already entered and tested. All you have to do is fill in the parameters highlighted in yellow and the answer will appear in the green cell.

5.2 Parallel Filaments

Another derivation allows for longitudinal displacement between the two filaments as shown in Figure 5-2.

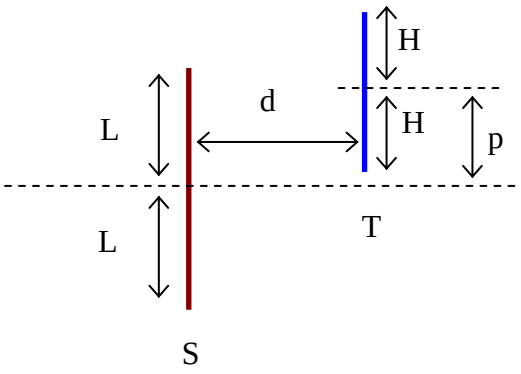

Figure 5-2 Parallel Filaments

5.2.1 Derivation

The derivation begins by writing down the wire form of the New Induction model.

$$1)\ V_K = -K_M \int_S \int_T \left(\frac{dI_S}{dt} \right) \frac{d\mathbf{L}_S \bullet d\mathbf{L}_T}{|\mathbf{r}|}$$

Then solve for DC mutual inductance

$$2)\ M_0 = K_M \int_S \int_T \frac{d\mathbf{L}_S \bullet d\mathbf{L}_T}{|\mathbf{r}|}$$

The distance (r) between source and target fragments is

$$3)\ r = \sqrt{(T + p - S)^2 + d^2}$$

Because the wires are parallel, we can drop the dot product. Also, for the sake of simplicity, we parameterize the source from –L to +L and the target from –H to +H. This is done to eliminate carrying along a plethora of T/2 and S/2 terms. The equation then becomes

4) $$M_0 = K_M \int_{S=-L}^{+L} \int_{T=-H}^{+H} \frac{dSdT}{\sqrt{(T+p-S)^2 + d^2}}$$

We begin hammering through the integration by substituting U=(T+p-S). This gives dU/dT=1, lower integration limit=(-H+p-S), upper=(H+p-S) and

5) $$M_0 = K_M \int_{S=-L}^{+L} \int_{U=(-H+p-S)}^{(H+p-S)} \frac{dSdU}{\sqrt{U^2 + d^2}}$$

Using form 157 (CRC tables edition 28)

6) $$M_0 = K_M \int_{S=-L}^{+L} \left[\begin{array}{l} \ln\left((H+p-S) + \sqrt{(H+p-S)^2 + d^2} \right) \\ -\ln\left((-H+p-S) + \sqrt{(-H+p-S)^2 + d^2} \right) \end{array} \right] dS$$

This can be restated as

7) $$M_0 = K_M \left[\begin{array}{l} \int_{S=-L}^{+L} \ln\left((H-S+p) + \sqrt{(H-S+p)^2 + d^2} \right) dS \\ -\int_{S=-L}^{+L} \ln\left(-(H+S-p) + \sqrt{(H+S-p)^2 + d^2} \right) dS \end{array} \right]$$

Continuing with the upper integrand first

8) $$K_M \int_{S=-L}^{+L} \ln\left((H-S+p) + \sqrt{(H-S+p)^2 + d^2} \right) dS$$

Substitute U=(H-S+p) which gives dU/dT=-1, lower limit=(H+L+p) and upper limit (H-L+p).

9) $$-K_M \int_{U=H+L+p}^{H-L+p} \ln\left(U+\sqrt{U^2+d^2}\right)dU$$

Using form 511 (CRC tables edition 28)

10) $$-K_M \left[U\ln\left(U+\sqrt{U^2+d^2}\right)-\sqrt{U^2+d^2}\right]_{H+L+p}^{H-L+p}$$

11) $$K_M\left[\begin{array}{l}-(H-L+p)\ln\left((H-L+p)+\sqrt{(H-L+p)^2+d^2}\right)+\sqrt{(H-L+p)^2+d^2}\\+(H+L+p)\ln\left((H+L+p)+\sqrt{(H+L+p)^2+d^2}\right)-\sqrt{(H+L+p)^2+d^2}\end{array}\right]$$

Next we perform the lower integration of step 7

12) $$M_0=-K_M\int_{S=-L}^{+L}\ln\left(-(H+S-p)+\sqrt{(H+S-p)^2+d^2}\right)dS$$

Substitute U=-(H+S-P). This yields dU/dS=-1, Lower integration limit=-(H-L-p) and upper integration limit=-(H+L-p) thus:

13) $$M_0=K_M\int_{U=-(H-L-p)}^{-(H+L-p)}\ln\left(U+\sqrt{(-U)^2+d^2}\right)dS$$

Which is the same as

14) $$M_0=K_M\int_{U=-(H-L-p)}^{-(H+L-p)}\ln\left(U+\sqrt{U^2+d^2}\right)dS$$

Using form 511 (CRC tables edition 28)

15) $$K_M\left[U\ln\left(U+\sqrt{U^2+d^2}\right)-\sqrt{U^2+d^2}\right]_{-(H-L-p)}^{-(H+L-p)}$$

16) $$K_M\left[\begin{array}{l}-(H+L-p)\ln\left(-(H+L-p)+\sqrt{(H+L-p)^2+d^2}\right)-\sqrt{(H+L-p)^2+d^2}\\+(H-L-p)\ln\left(-(H-L-p)+\sqrt{(H-L-p)^2+d^2}\right)+\sqrt{(H-L-p)^2+d^2}\end{array}\right]$$

Combining the results from steps 11 and 16

17)

$$M_0 = K_M \left[\begin{array}{l} +(H+L+p)\ln\left((H+L+p)+\sqrt{(H+L+p)^2+d^2}\right)-\sqrt{(H+L+p)^2+d^2} \\ -(H+L-p)\ln\left(-(H+L-p)+\sqrt{(H+L-p)^2+d^2}\right)-\sqrt{(H+L-p)^2+d^2} \\ -(H-L+p)\ln\left((H-L+p)+\sqrt{(H-L+p)^2+d^2}\right)+\sqrt{(H-L+p)^2+d^2} \\ +(H-L-p)\ln\left(-(H-L-p)+\sqrt{(H-L-p)^2+d^2}\right)+\sqrt{(H-L-p)^2+d^2} \end{array} \right]$$

5.2.2 "Algorithmification"

Turning the Parallel wire equations into a computer or spreadsheet algorithm is quite simple. We first make the following substitutions:

$$A = H + L + p$$
$$B = H + L - p$$
$$C = H - L + p$$
$$D = H - L - p$$

Yielding

$$M_0 = K_M \left[\begin{array}{l} +A\ln\left(A+\sqrt{A^2+d^2}\right)-\sqrt{A^2+d^2} \\ -B\ln\left(-B+\sqrt{B^2+d^2}\right)-\sqrt{B^2+d^2} \\ -C\ln\left(C+\sqrt{C^2+d^2}\right)+\sqrt{C^2+d^2} \\ +D\ln\left(-D+\sqrt{D^2+d^2}\right)+\sqrt{D^2+d^2} \end{array} \right]$$

Then substitute

$$AA = \sqrt{A^2 + d^2}$$
$$BB = \sqrt{B^2 + d^2}$$
$$CC = \sqrt{C^2 + d^2}$$
$$DD = \sqrt{D^2 + d^2}$$

Then

$$M_0 = K_M \begin{bmatrix} +A\ln(A + AA) - AA \\ -B\ln(-B + BB) - BB \\ -C\ln(C + CC) + CC \\ +D\ln(-D + DD) + DD \end{bmatrix}$$

Finally, remember that

$$S = 2L$$
$$T = 2H$$
Thus
$$L = S/2$$
$$H = T/2$$

So that

$$A = T/2 + S/2 + p$$
$$B = T/2 + S/2 - p$$
$$C = T/2 - S/2 + p$$
$$D = T/2 - S/2 - p$$

The C++ Algorithm

```
DOUBLE DC_mutual_parallel_filaments(DOUBLE S, DOUBLE T, DOUBLE d, DOUBLE p){
        DOUBLE H,L,A,B,C,D,AA,BB,CC,DD,AAA,BBB,CCC,DDD, result;
    H=T/2;
    L=S/2;
    A=H+L+p;
    B=H+L-p;
    C=H-L+p;
    D=H-L-p;
    DD=d*d;            // temporary use of DD
    AA=sqrt(A*A+DD);
    BB=sqrt(B*B+DD);
    CC=sqrt(C*C+DD);
    DD=sqrt(D*D+DD);
    AAA=A+AA;
    BBB=-B+BB;
    CCC=C+CC;
    DDD=-D+DD;
    if(AAA>0.0 && BBB>0.0 && CCC>0.0 && DDD>0.0){    // Test to avoid exception
        result=A*log(AAA)-AA;
        result+=-B*log(BBB)-BB;
        result+=-C*log(CCC)+CC;
        result+=D*log(DDD)+DD;
        result*=Km;
    }else{
       // Place warning here that illegal parameters detected ;
        result=-DBL_MAX;      //return near infinity
    }
    return result;
}
```

The Excel Algorithm

Accompanying this text is an EXCEL (NIA1.XLS) spread sheet that contains the Parallel Filament equation already entered and tested. All you have to do is fill in the parameters highlighted in yellow and the answer will appear in the green cell.

6 Antennae Modeling

The New Electromagnetic models are much simpler to apply to radio communication antennae modeling than the classical models (Maxwell's equations). Many classical textbooks often cite that antennae theory is more art or black magic than science. Take for example the following passages:

"People who work in antennae technology often say that antennas are built with a combination of art, science and a little black magic." --- From page 661 of the text "Applied Electronic Communications" by Robert Kellejian.

"The three equations [approximations for dipole field energy derived from Maxwell's equations] are indicative of the reason why problems involving antennas are solved by experimental rather than theoretical methods."—From "Engineering Electromagnetics" by William H. Hayt Jr.

The mentioned problems with classical antennae field theory are due to a number of problems:

1) Classical models are unnecessarily complicated.
2) Maxwell's equations are "Point equations"; therefore they are only an approximation for a non-point antennae system.
3) Classical models only describe a toroid shaped magnetic field; a spherical magnetic field is required to properly compute an antenna radiation pattern (as will be shown in this text).
4) In classical electromagnetic theory, the E-field is required for the calculation. In New Electromagnetism, the E-field is a short range effect that can be omitted with little effect to the accuracy of the result.

This text shows that antenna radiation calculations using the New Electromagnetic models are an exact science, not black magic or art.

The derivation contained in the following text shows that electromagnetic radiation is a purely magnetic phenomenon. Although we will use the terms transverse wave and longitudinal wave in the derivation, electromagnetic radiation is truly a spherical wave phenomenon.

This text applies the New Electromagnetic principles to a standard half wave dipole system. Applications beyond this are an academic matter once the fundamental concepts are understood.

6.1 The Half Wave dipole antenna

A standard half wave dipole consists of two quarter wave radiators arranged as shown in Figure 6-1

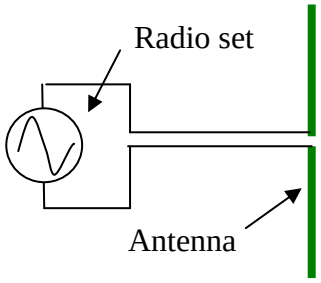

Figure 6-1

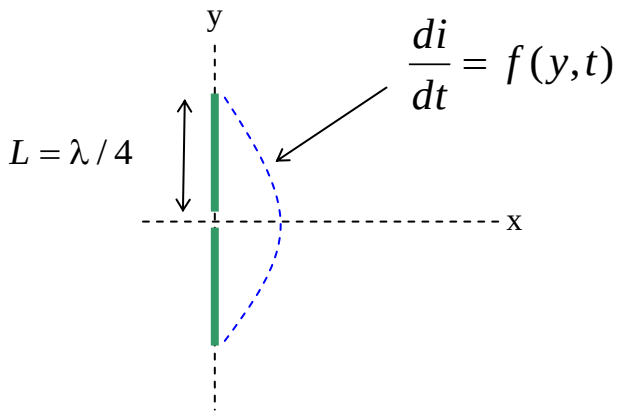

Figure 6-2 Parameterization of antenna

In classical electromagnetic theory, the dipole is modeled by considering all field effects. The New Electromagnetic models teach us that the Electric and Motional fields are inverse square effects while the Inertial is an inverse effect. This means that beyond a certain distance (the Far Field is the term used by ARRL) from the dipole, the Inertial component (New Induction) is the predominant effect. This section derives a dipole model from New Induction that agrees very accurately with the known behavior of dipole antennas.

Since the New Induction deals with current change, we need a relationship that shows the current change in a dipole as a function of time (t) and position (y); see Figure 6-2.

First we consider that the base of the antenna is driven by a time changing current source with the following characteristics

1) $i(t) = I_0 \cos(2\pi ft)$

Since we need to deal only with the change in antenna current we take the derivative of step 1:

2) $\frac{di}{dt} = -2\pi f I_0 \sin(2\pi f t)$

Since it our objective to derive the equation of a dipole operated in the quarter wave mode, the current-change along the length of the dipole will be in phase; however, the amplitude will diminish toward the ends of the dipole. This is analogous to a guitar string vibrating at its fundamental frequency. In such a guitar string, each element moves in phase; however, the magnitude of vibration diminishes to zero where the string is mounted to the guitar. Therefore, we apply an "envelope" in the form of a cosine as shown:

$$\frac{di}{dt} = -2\pi f I_0 \sin(2\pi f t)\cos\left(\frac{y\pi}{2L}\right) \text{ for } L = \frac{\lambda}{4} = \frac{C}{4f}$$

Equation 6-1: Source current model

Step 4 is the critical part of this derivation. The distribution of current (specifically current change) in the radiating elements affects the shape of the radiation pattern that is sent into space (to be demonstrated shortly).

We add another level of detail to Equation 6-1 by accounting for the propagation delay from any fragment of the dipole to an arbitrary point in space using the assumption that the effect travels at the speed of light (C). Since the distance from a source fragment to target fragment is defined in New Electromagnetism as:

3) $|\mathbf{r}|$ and

4) time=distance/velocity then

5) $t_R = \frac{|\mathbf{r}|}{C}$ This is called the time retardation factor.

This time retardation factor is then subtracted from the source time thus:

$$\frac{di}{dt} = -2\pi f I_0 \sin\left(2\pi f\left(t - \frac{|\mathbf{r}|}{C}\right)\right)\cos\left(\frac{y\pi}{2L}\right) \text{ for } L = \frac{\lambda}{4} = \frac{C}{4f}$$

Equation 6-2 Retarded time source current model

We could do the "electrical engineering thing" by converting the above expression to phasor notation; however, this would only serve to alienate a good portion of readers who probably don't know phasor notation or have since forgotten it.

With two good expressions for source current distribution, we now put them to use.

6.1.1 Energy received at transverse position

In this section we use Equation 6-1 to determine the V_K (emf) receive by another dipole (the target) which is parallel to the source and located along the transverse axis as show in Figure 6-3.

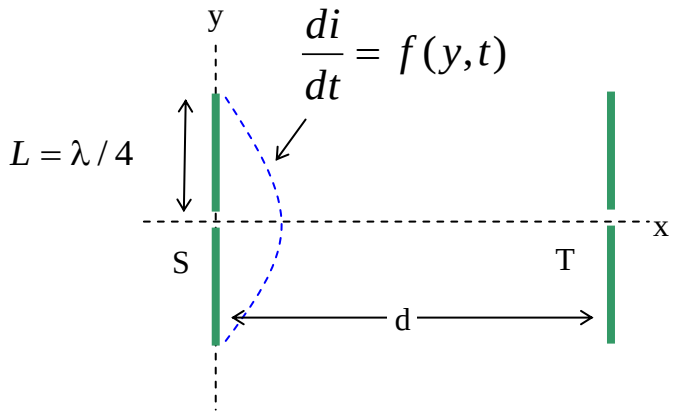

Figure 6-3

We start with the wire form of New Induction:

$$1)\ V_K = -K_M \int_S \int_T \left(\frac{dI_S}{dt} \right) \frac{d\mathbf{L}_S \bullet d\mathbf{L}_T}{|\mathbf{r}|}$$

Since the target is parallel and sufficiently far away, the effect felt by the target is going to be substantially uniform over its length; therefore, we simplify the problem as follows:

$$2)\ V_K = \frac{-2K_M L}{d} \int_S \left(\frac{dI_S}{dt} \right) dL_S$$

We can also assume that the propagation delay from each source fragment to each target fragment is substantially the same; therefore we use Equation 6-1 to model the current in the source since it does not account for propagation delay.

3) $V_K = \frac{2K_M L}{d} 2\pi f I_0 \sin(2\pi f t) \int_{y=-L}^{+L} \cos\left(\frac{y\pi}{2L}\right) dy$

Then perform the integration

4) $V_K = \frac{8K_M L^2}{d} f I_0 \sin(2\pi f t)\left[\sin\left(\frac{\pi}{2}\right) - \sin\left(\frac{-\pi}{2}\right)\right]$

5) $V_K = \frac{16K_M L^2 f}{d} I_0 \sin(2\pi f t)$

Since the radiators operate in the quarter wave mode, substitute $L = \frac{\lambda}{4} = \frac{C}{4f}$ and

$V_K = \frac{K_M C^2}{fd} I_0 \sin(2\pi f t)$ (for half-wave dipoles only)

Equation 6-3: Traverse Dipole Equation

The above equation is the kinetic voltage (emf) induced in a dipole receiver. Unlike the classical derivations which are quite lengthy and obscure, this derivation of coupling between emitter and receiver is quite simple.

In the above equation it is observed that the received signal magnitude diminishes with both distance and frequency, this must mean that low frequency signals should travel farther than high frequency signals; this is indeed the case with observed phenomena.

Since New Induction is a spherical model, one might incorrectly assume that the received energy with the target held parallel at the axial position would be the same. We shall look at this case next.

6.1.2 Energy at the longitudinal position

The following diagram is another view of Figure 6-3 with the origin rotated 90 degrees to the right and the target dipole moved to an axial (or longitudinal) position relative to the emitter. The receiver is sufficiently far away such that the inverse square effects (Electric and Motional) can be ignored.

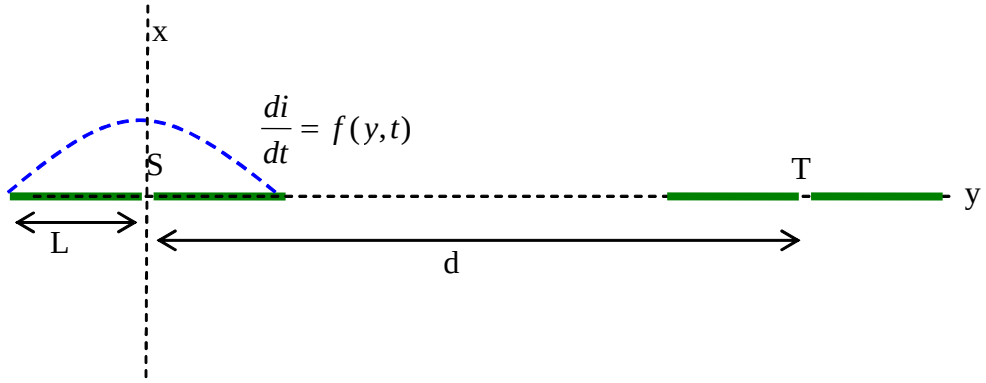

Figure 6-4 Longitudinal effects

In the previous derivation, the energy emitted from each fragment of the source arrives at the target at substantially the same time; therefore, the constructive and destructive overlap of the transmitted energy was ignored.

In this case, by accounting for the constructive and destructive affects, we will show that the received V_K is half of that received in the transverse case. This corresponds to ¼ the power or -6dB difference in gain. The classical electromagnetic models (Maxwell's Equations) predict no power at all (effectively $-\infty$dB) in the longitudinal direction while the American Radio Relay League (ARRL) measured value is -9dB (a comparative study follows in section 6.1.3). Before we get too far off track, let's solve the longitudinal equation for the dipole:

Starting with the wire form of New Induction

$$1)\ V_K = -K_M \int_S \int_T \left(\frac{dI_S}{dt} \right) \frac{d\mathbf{L}_S \bullet d\mathbf{L}_T}{|\mathbf{r}|}$$

And the retarded time source current model (Equation 6-2)

2) $\frac{di}{dt} = -2\pi f I_0 \sin\left(2\pi f\left(t - \frac{|\mathbf{r}|}{C}\right)\right)\cos\left(\frac{y\pi}{2L}\right)$

Substitute step 2 into step 1:

4) $V_K = 2\pi f I_0 K_M \int_S \int_T \sin\left(2\pi f\left(t - \frac{|\mathbf{r}|}{C}\right)\right)\cos\left(\frac{y\pi}{2L}\right)\frac{d\mathbf{L}_S \bullet d\mathbf{L}_T}{|\mathbf{r}|}$

Let us use the variable y to parameterize the source and the variable l to parameterize the target. Thus:

5) $V_K = 2\pi f I_0 K_M \int_{l=-L}^{+L} \int_{y=-L}^{+L} \sin\left(2\pi f\left(t - \frac{d+l-y}{C}\right)\right)\cos\left(\frac{y\pi}{2L}\right)\frac{dydl}{d+l-y}$

Since the source and target are considerably far away, we can assume that the denominator on the far right is dominated by the distance d; therefore, we drop the l-y and move d outside the integration as follows

6) $V_K = \frac{2\pi f I_0 K_M}{d} \int_{l=-L}^{+L} \int_{y=-L}^{+L} \sin\left(2\pi f\left(t - \frac{d+l-y}{C}\right)\right)\cos\left(\frac{y\pi}{2L}\right)dydl$

We will perform the integration with respect to y first. To make the integration simpler we perform Euler expansion of the sine and cosine

7) $V_K = \frac{2\pi f I_0 K_M}{d} \int_{l=-L}^{+L} \int_{y=-L}^{+L} \frac{1}{4j}\left(e^{j2\pi f\left(t-\frac{d+l-y}{c}\right)} - e^{-j2\pi f\left(t-\frac{d+l-y}{c}\right)}\right)\left(e^{j\frac{y\pi}{2L}} + e^{-j\frac{y\pi}{2L}}\right)dydl$

After a bit of rearranging

8) $V_K = \frac{\pi f I_0 K_M}{2jd} \int_{l=-L}^{+L} \int_{y=-L}^{+L} \left(e^{j2\pi f\left(t-\frac{d}{C}-\frac{l}{C}+\frac{y}{C}\right)} - e^{-j2\pi f\left(t-\frac{d}{C}-\frac{l}{C}+\frac{y}{C}\right)}\right)\left(e^{j2\pi f\frac{y}{C}} + e^{-j2\pi f\frac{y}{C}}\right)dydl$

Multiplying

$$9)\ V_K = \frac{\pi f I_0 K_M}{2jd} \int_{l=-L}^{+L} \int_{y=-L}^{+L} \begin{pmatrix} e^{j2\pi f(t-\frac{d}{C}-\frac{l}{C}+2\frac{y}{C})} \\ -e^{-j2\pi f(t-\frac{d}{C}-\frac{l}{C})} \\ +e^{j2\pi f(t-\frac{d}{C}-\frac{l}{C})} \\ -e^{-j2\pi f(t-\frac{d}{C}-\frac{l}{C}+2\frac{y}{C})} \end{pmatrix} dydl$$

Integrate

$$10)\ V_K = \frac{\pi f I_0 K_M}{2jd} \int_{l=-L}^{+L} \begin{pmatrix} \frac{C}{j4\pi f} e^{j2\pi f(t-\frac{d}{C}-\frac{l}{C}+2\frac{y}{C})} - ye^{-j2\pi f(t-\frac{d}{C}-\frac{l}{C})} \\ +ye^{j2\pi f(t-\frac{d}{C}-\frac{l}{C})} + \frac{C}{j4\pi f} e^{-j2\pi f(t-\frac{d}{C}-\frac{l}{C}+2\frac{y}{C})} \end{pmatrix}_{-L}^{L} dl$$

Before substituting the integration limits, reconstitute the trig functions

$$11)\ V_K = \frac{\pi f I_0 K_M}{d} \int_{l=-L}^{+L} \begin{pmatrix} +y\sin\left(2\pi f(t-\frac{d}{C}-\frac{l}{C})\right) \\ -\frac{C}{8\pi f}\cos\left(2\pi f(t-\frac{d}{C}-\frac{l}{C}+2\frac{y}{C})\right) \end{pmatrix}_{-L}^{L} dl$$

Substitute limits and simplify:

$$12)\ V_K = \frac{2\pi f I_0 K_M L}{d} \int_{l=-L}^{+L} \sin\left(2\pi f(t-\frac{d}{C}-\frac{l}{C})\right) dl$$

Next perform integration of l:

$$13)\ V_K = \frac{2\pi f I_0 K_M L}{d} \left[\frac{C}{2\pi f}\cos\left(2\pi f(t-\frac{d}{C}-\frac{l}{C})\right)\right]_{-L}^{L}$$

After substitution of limits and simplification

$$V_K = \frac{I_0 K_M C^2}{2fd}\cos\left(2\pi f(t-\frac{d}{C})\right)$$

Equation 6-4: Longitudinal Dipole Equation

As stated previously, the magnitude of the equation is ½ of that in the transverse case. The ARRL measures the ratio in received signal magnitude between transverse and longitudinal directions to be $\frac{1}{2.828}$. Classical theory predicts no energy at all on the longitudinal direction. We will show a comparative plot of the different models in section 6.1.3

6.1.3 General Dipole Radiation pattern

In this section, we derive the V_K present at an arbitrary distant point from the source dipole. From this we plot the propagation pattern of a simple dipole to see if it corresponds to measured results.

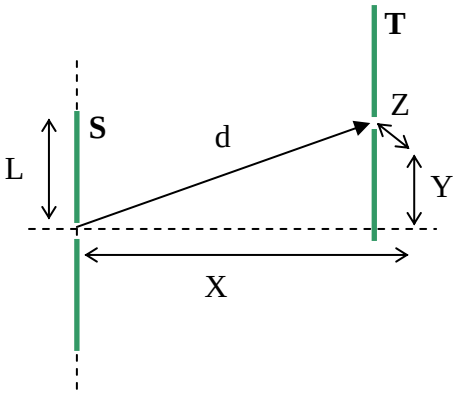

Figure 6-5 Dipole located at any arbitrary point (X,Y,Z)

Note: the following only derives the equation in X and Y; the software algorithms that are provided in this text account for X, Y, Z and ground effects.

We set up the problem by locating a target dipole at an arbitrary distance from the source dipole. For simplicity, the target is kept parallel to the source such that maximum coupling is achieved.

The range from a fragment of the source to a fragment of the target is:

1) $|\mathbf{r}| = \sqrt{X^2 + (Y - y)^2}$

Starting from step 4 of the previous section

2) $V_K = 2\pi f I_0 K_M \int_S \int_T \sin 2\pi f \left(t - \frac{|\mathbf{r}|}{c} \right) \cos\left(\frac{y\pi}{2L} \right) \frac{d\mathbf{L}_S \bullet d\mathbf{L}_T}{|\mathbf{r}|}$

Substituting 1 into 2

$$3)\ V_K = 2\pi f I_0 K_M \int_{y=-L}^{+L} \int_T \sin 2\pi f \left(t - \frac{\sqrt{X^2 + (Y-y)^2}}{c} \right) \cos\left(\frac{y\pi}{2L}\right) \frac{dy dL_T}{\sqrt{X^2 + (Y-y)^2}}$$

The above integral is too difficult to solve by hand; instead, we have provided a numerical integration algorithm shown in a following box titled Code Fragment 1 on page 37.

The algorithm shown in Code Fragment 1 is actually more sophisticated than the above equations since it provides for the Z axis as well as ground effects. The ground effects are determined using the inductive MOI shown in section 10.1 which is similar to the Perfect-Earth technique as documented in the American Radio Relay League (www.arrl.com) Antenna Book (chapter 3: The Effect of Ground in the Far Field). Obviously the Earth is not a perfectly conductive body so the ground effects are only approximate. A later book in the New Electromagnetism Application Series covers electromagnetic reflections and refraction in great detail and will provide a more suitable ground effect model for radio.

In the following computer plot, the output of the algorithm is compared against other methods for predicting the Far Field radiation pattern of a Half-Wave dipole. In the chart the dipole is located at the origin and parallel to the horizontal line.

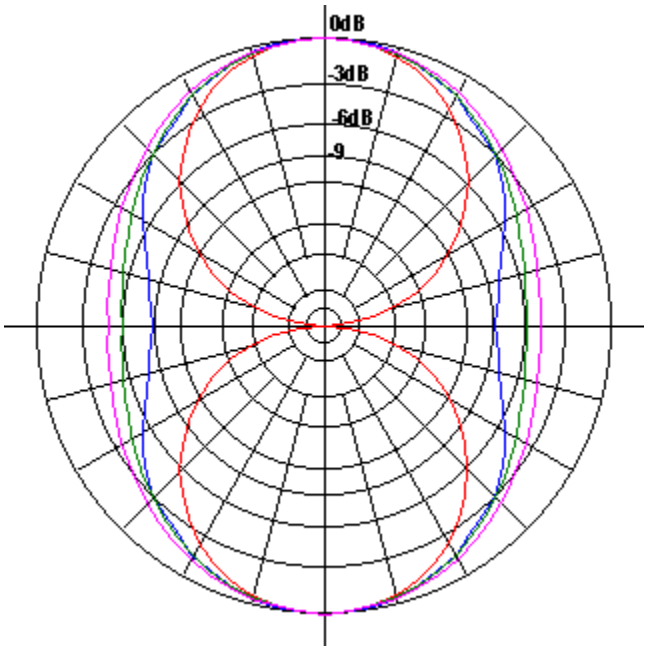

Figure 6-6 Radiation Patterns (All outputs are normalized)

In the above chart, the red plot is the radiation pattern predicted by classical theory. From the plot you will notice that no energy is transmitted in the longitudinal directions. The reason why no effects are predicted in the longitudinal direction is that classical theory only provides for a transverse magnetic field.

The blue trace is the measured radiation pattern of a half-wave dipole found in the ARRL Antenna Book (chapter 6, figure 3, page 6-3). Since this trace is empirical data, ground effects are included.

The green trace is the output of the algorithm shown in Code Fragment 1 with the ground effects loop commented out. This represents the exact results of the hand derived equations shown in previous sections. If you compare Equation 6-3 to Equation 6-4 you will notice that there is 6dB difference between the results. This 6dB difference between the longitudinal and transverse directions is reflected in the chart as well. The parameters used for the algorithm are lambda=1; z=0; sqrt(x*x+y*y) =100*lambda, t=see note following code fragment.

The fuchsia trace shows the algorithm with ground effects included. The dipole is ¼ lambda above ground and the sensing position is 25 degrees from the horizontal at a range of 100 lambdas.

Code Fragment 1

```
// This is dipole-to-dipole with ground effects
// The height of source dipole is Quarter wave above ground (L4)
// The height of target is source.z + z (L4+z) above ground
// To remove ground effects, comment out the second for(i) loop
// the returned result is in the form of Vk/Io
DOUBLE dipole_to_dipole_w_ground(DOUBLE x, DOUBLE y, DOUBLE z, DOUBLE lambda, DOUBLE t){
    DOUBLE result=0;
    int i,k;
    DOUBLE L4,dl,f,rx,ry,rz,rt,S,T,d, demf, KK, KS, KT;
    L4=lambda/4;              //quarter wave
    dl=L4/N;                  // Calculate dL
    f=C/lambda;               // Calculate frequency
    KK=1e-7*dl*dl*2*M_PI*f;   // Preprare constant

    // first take effects from source to target
    for(i=-N; i<N; i++){
        S=i*dl+dl/2;          // source dipole element
        KS=cos(S/L4*M_PI/2);  // calculate current envelope
        for(k=-N; k<N; k++){
            T=k*dl+dl/2;      // target dipole position
            ry=T-S+y;
            rx=x;
            rz=z;
            d=sqrt(rx*rx+ry*ry+rz*rz);
            rt=t-fabs(d/C);
            demf=KK*sin(2*M_PI*f*rt)*KS/d;
            result+=demf;
        }
    }

    // now consider ground effects
    // Z is 2*L4 + z
    for(i=-N; i<N; i++){
        S=i*dl+dl/2;          // source dipole element
        KS=cos(S/L4*M_PI/2);  // calculate current envelope
        for(k=-N; k<N; k++){
            T=k*dl+dl/2;      // target dipole position
            ry=T-S+y;
            rx=x;
            rz=2*L4+z;
            d=sqrt(rx*rx+ry*ry+rz*rz);
            rt=t-fabs(d/C);
            demf=KK*sin(2*M_PI*f*rt)*KS/d;
            result-=demf;
        }
    }
    return result;
}
```

Constants used in the above algorithm
#define N 20 // This is number of increments in each radiator
#define C 3e8 // speed of light

The above algorithm provides instantaneous values; thus the answer obtained is modulated by the phase of the signal. In order to find the peak value at any given location, the following algorithm is used. This algorithm varies the source phase over 1/2 period in order to find the peak value at the receiver. The algorithm divides the signal period by twelve, then indexes through the first eight points to find the max amplitude. For your application, you may have to increase the resolution of the search.


```
//Simple routine to find local maximum
// amax, lambda, tmp, dp are DOUBLE
// k is integer

    amax=0;
    dp=lambda/12;
    for(k=0;k<7;k++){
        tmp= dipole_to_dipole_w_ground(X,Y,Z,lambda,k*dp);
        amax=max(amax,fabs(tmp));
    }
```

6.1.4 Conclusion

This section utilizes the same simplifications used in the classical derivation of dipole modeling and achieved more accurate results in a strait-forward manner. The most obvious simplification is the modeling of the charge behavior in the source antenna. This model for the source charge behavior is found in many classical electromagnetic texts (see "Electromagnetic Fields and Waves" by Paul Lorrain; chapter 39 as example). The key error in the source approximation (which is well known) is that it does not account for the energy loss due to radiation. More accurate modeling of charge behavior in the source will yield more accurate results; however, for many applications, the accuracy of the methods shown in this section is sufficient. The accuracy is certainly better than the classical methods.

The New Electromagnetic Dipole model gives the instantaneous kinetic voltage received in the target. Because the target is a resonant circuit (hopefully) the actual voltage detected in the receiver will be amplified what is called Q-rise. Q-rise is well described in the classical literature.

7 Spherical Wave Model

In chapter 6 we employed the New Induction model to accurately calculate the kinetic voltage induced in a target antenna. The answer obtained from New Electromagnetism was far more accurate than the answer provided for by classical electromagnetic theory. The primary reason for this is that classical theory only considers magnetism to be a transverse field. New Electromagnetism teaches that magnetism is a spherical field (which includes both transverse and longitudinal components). Only by considering both the longitudinal and transverse components can accurate radiation patterns be predicted.

Classical electromagnetic wave theory requires both an E-field and B-field for the propagation of effects. We have shown in other publications that an electric field can not be "source-less" as asserted by Maxwell's version of Faraday's Law. We also show that Maxwell's displacement current term violates Einstein's assertion that a magnetic field must follow its source (In New Magnetism the source can only be charges); therefore magnetic fields can not be induced by time varying electric flux. With the above assertions, the plane wave model derived by Maxwell can no longer be considered viable.

New Electromagnetism teaches us that electromagnetic radiation is purely a magnetic field phenomenon since only the New Induction model is required for calculating radiation effects. Since New Induction shows that energy is emitted in all directions from an accelerating charge, then electromagnetic radiation is actually a spherical wave phenomenon and not the transverse wave phenomenon as predicted in classical theory.

The underlying mechanism that explains how the acceleration of a charge causes an effect on another charge at some distant point can not be directly derived from the electromagnetic equations (see Rules of Nature—ron.pdf). The derivations of the underlying mechanisms are a topic of the Ethereal Mechanics series of books and papers.

8 Rectangular Loops

In this section we use the parallel filament equation to calculate the mutual inductance between two rectangular loops of wire (air core). The two loop system has many useful applications to include metal detectors and position sensing.

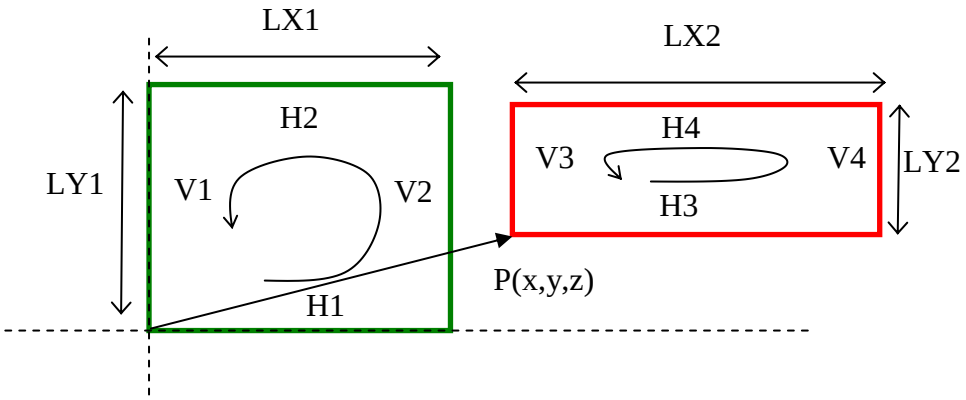

Figure 8-1 Two rectangular loops

This application considers two rectangular loops of wire with any number of turns. The lower left hand corner of the first loop is located at the origin (0,0,0) and the lower left hand corner of the second loop is located at any arbitrary position in space except where the filaments would co-exists. For the sake of discussion we call the green loop the source and the red loop the target.

The following variables are introduced
LX1=horizontal length of loop 1
LY1=vertical length of loop 1
LX2=horizontal length of loop 2
LY2=vertical length of loop 2
PX2=horizontal position of lower left of loop 2
PY2=vertical position of lower left of loop 2
PZ2=Z position of lower left of loop 2
N1=number of turns in loop1
N2=number of turns in loop2

The following are labels to help us identify the various segments:
V1, V2, V3 and V4 are the vertical segments of the loops.
H1, H2, H3, and H4 are the horizontal segments of the loops.

The circular arrows help us keep track of the direction of the segments around the loop; they are arbitrarily chosen in the counter-clockwise direction. If the side of the circular loop representing a segment is in the positive direction with respect to the axes, then the direction of the segment is positive (example: segment H1 is positive). If the side of the circular loop is in the negative direction, then the direction of the segment is negative (Example: H2 is negative). If you are not clear on the meaning of the arrows, it will become clear as this derivation progresses; essentially, the arrows are used in a manner identical to loop analysis.

Since New Induction shows that orthogonal segments do not affect each other, only the interactions between parallel segments need be calculated.

Let us first take a look at one such interaction as an example. The first interaction is the V_K (emf) induced in H3 from the current change in H1 (written in shorthand as H1→H3).

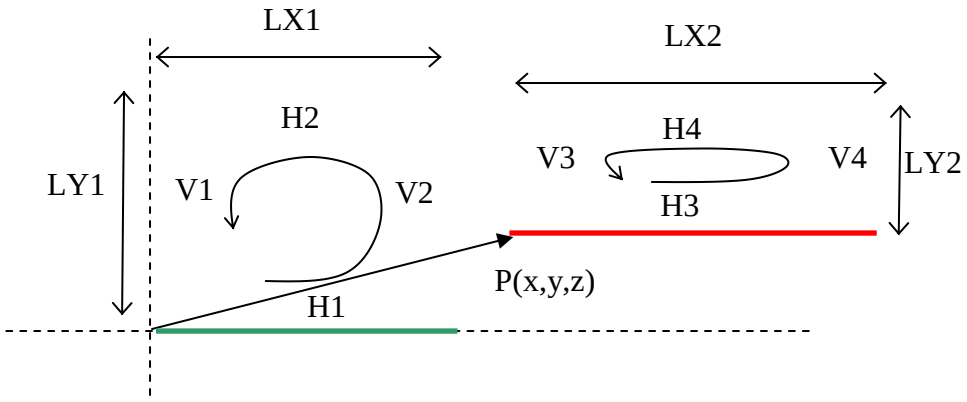

Figure 8-2 The interaction between H1 and H3

The H1→H3 interaction is shown in Figure 8-2, we deduce the parameters required for the parallel filament equation. The sign of the result is positive since both segments are in the same direction (relative to the circular arrows drawn within).

Algorithm Parameter	Use
S	+LX1 (Positive since this segment is in positive x direction)
T	+LX2 (Positive since this segment is in positive x direction
d	sqrt(PY2*PY2+PZ2*PZ2)
p	LX2/2+PX2-LX1/2

As another example, the H1→H4 interaction is considered (referring to Figure 8-3).

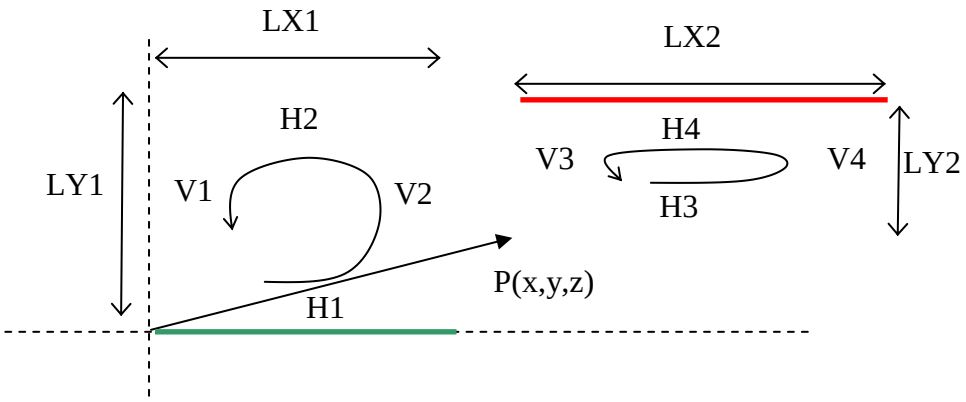

Figure 8-3 The interaction between H1 and H4

The H1→H4 interaction is calculated from the Parallel Filament equation using the following parameters:

Algorithm Parameter	Use
S	+LX1 (positive since this segments direction is positive around the loop)
T	-LX2 (negative since this segments direction is negative)
d	sqrt((PY2+LY2)^2+PZ2*PZ2)
p	LX2/2+PX2-LX1/2

The above procedures are performed for all interactions and the results summed to find to the total "single turn mutual inductive linkage". The single turn linkage is the multiplied by N1 and N2 to arrive at the total linkage.

The complete list of 8 interactions to be calculated is:

H1→H3
H1→H4
H2→H3
H2→H4
V1→V3
V1→V4
V2→V3

V2→V4

Instead of running each set of parameters through the Parallel Filament equations, we have done the work for you in the accompanying EXCEL spread sheet application.

The Excel Algorithm

The EXCEL spreadsheet application (NIA1.XLS) that accompanies this text contains a Rectangular Loops Algorithm which does all the work for you; all you have to do is enter the basic parameters highlighted in the yellow cells and the total mutual inductance is show in the cell highlighted in green.

8.1 Rectangular Loop Example

To test the results of the Rectangular Loops Algorithm (which uses the Parallel Filaments Algorithm), consider the following example

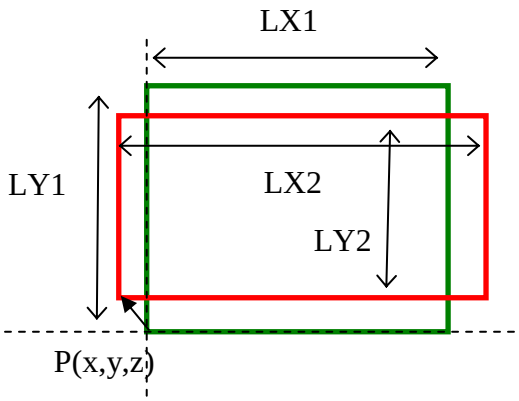

Figure 8-4 Example

Where
LX1=13cm (0.13m)
LY1=10cm (0.10m)
LX2=11cm (0.11m)
LY2=12cm (0.12m)
PX2=1cm (0.01m)
PY2=-1cm (-0.01m)
PZ2=0 (0)
N1=1
N2=1

Note: the above values must be converted to meters before entered into the spreadsheet. The spreadsheet comes with the above parameters already inserted.

The result is:

M_0=1.57764e-07 Henries

To test the results of the algorithm, we construct the loops from simple materials and measure the mutual inductance.

We begin by taping a sheet of paper to a flat board and then carefully penciling in loops of the appropriate dimensions. This is shown in the following photo; the pencil lines may be hard to see.

Figure 8-5

Next, apply contact cement along the lines and let the cement dry until it is tacky. Please follow the instruction on the contact cement label.

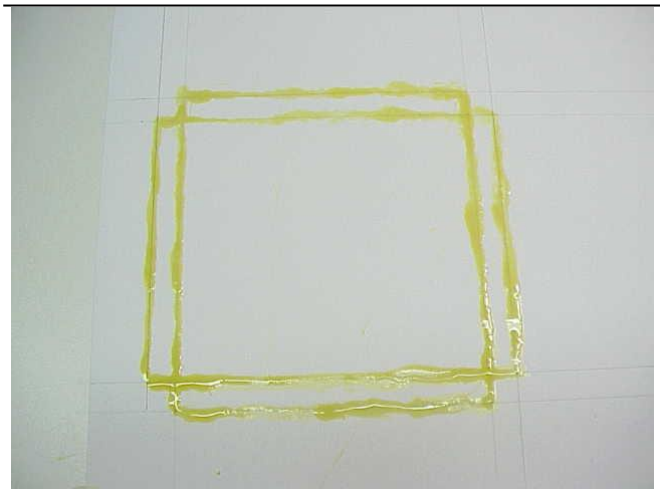

Figure 8-6 Application of contact cement

Then lay magnet or wire wrap wire onto the appropriate pencil marks; center the wire over the marks. Be careful, an error of 1mm will throw the results off by as much as 10% (you can test this by changing the parameters in the spreadsheet and observing the change in the result. Extend the wires of each rectangle from different corners and twist them together to form pigtails. Use tape to secure the pigtails.

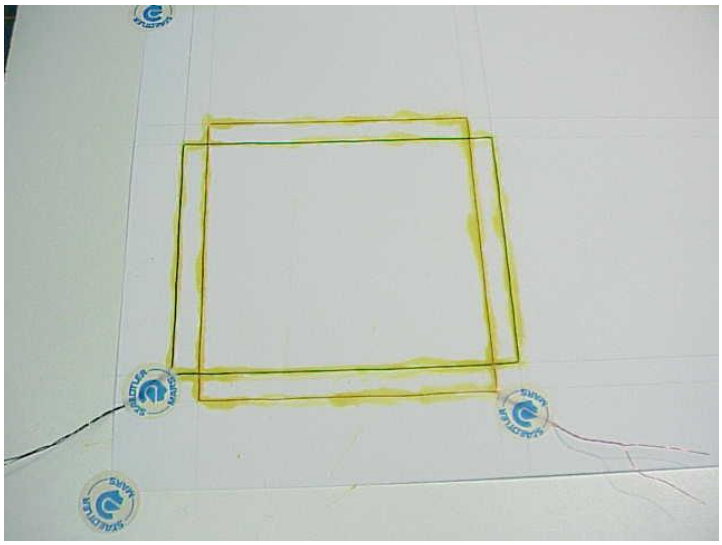

Figure 8-7

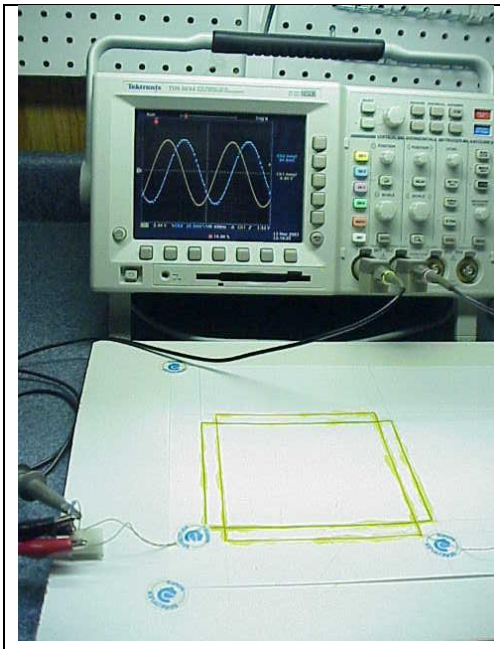

Figure 8-8

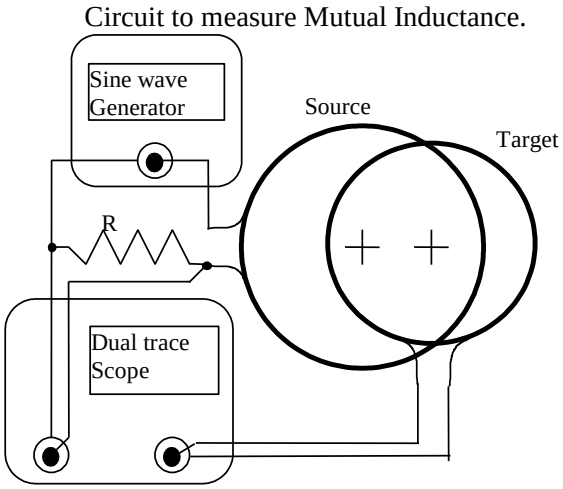

Figure 8-9 Circuit used to measure Mutual inductance (for any shape of loops)

The setup used to measure the mutual inductance (Figure 8-9) is the same used in the New Induction paper (except for the value of resistance).

Remember that the Mutual Inductance relates the kinetic voltage (emf) induced in the target loop to the current change in the source loop:

$$0) V_{KT}(t) = -M\frac{di_S(t)}{dt}$$

The current through the source loop is the voltage across the termination resistor divided by its resistance thus

$$1)\ I_S = \frac{V_R}{R} \text{ and}$$

$$2)\ \frac{dI_S}{dt} = \frac{1}{R}\frac{dV_R}{dt}$$

Since we are using a sinusoidal function generator

$$3)\ V_R = V_{RO}\sin(2\pi ft) \text{ then}$$

4) $\frac{dV_R}{dt} = 2\pi f V_{RO} \cos(2\pi ft)$

Substituting 4 into 2 yields

5) $\frac{dI_S}{dt} = \frac{V_{RO}}{R} 2\pi f \cos(2\pi ft)$

Substituting 5 into 0 yields:

6) $V_{KT}(t) = -M \frac{V_{RO}}{R} 2\pi f \cos(2\pi ft)$

Thus the Peak to Peak voltage amplitude of the target output is:

7) $V_{KT}(p-p) = M \frac{V_{R0}}{R} 4\pi f$

Since we have a high impedance load on the output of the target, the kinetic voltage will convert directly to potential voltage, thus

8) $V_T(p-p) = M \frac{V_{R0}}{R} 4\pi f$

The Peak-to-Peak voltage across the Source termination resistor is

9) $V_{RS}(p-p) = 2V_{R0}$ Rearranging yields

10) $V_{R0} = \frac{V_{RS}(p-p)}{2}$

Substituting 10 into 8

11) $M = \frac{V_T(p-p)}{V_{RS}(p-p)} \frac{R}{2\pi f}$

Step 11 is a relationship to calculate the mutual inductance between two loops based on peak-to-peak values measured with an oscilloscope.

The first test is conducted with a Tektronix APG310 Arbitrary function generator; the function output is selected for sine wave, 10V p-p and frequency of 500 KHz. The termination resistor is 49.9 ohms (1%). The oscilloscope output waveform (Figure 8-10) captures the results of this test. The violet trace (CH1) is the reading across the termination resistor and the cyan trace (CH2) is the output of the target loop.

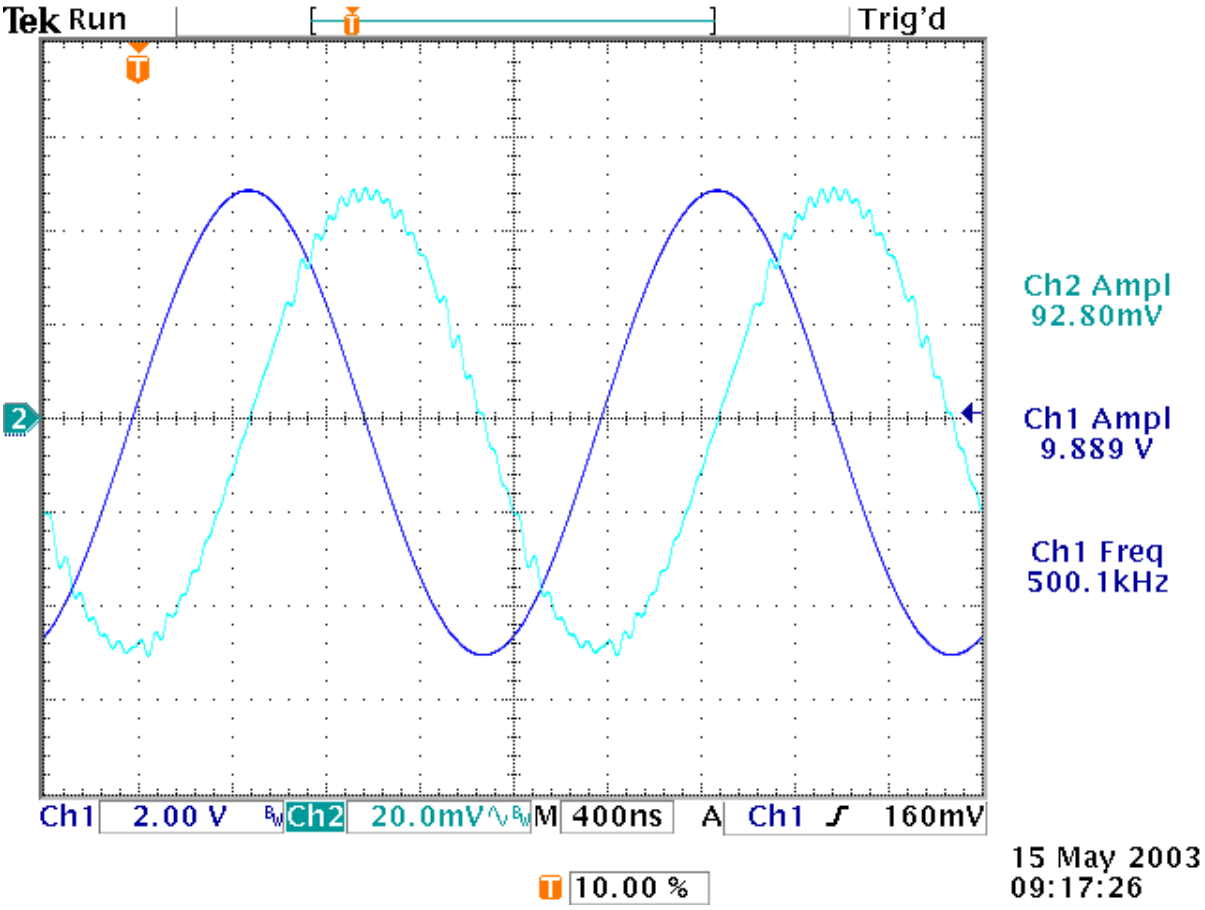

Figure 8-10 Using Tektronix AFG310 arbitrary function generator (Digital)

Using the relationship derived previously, we calculate the mutual inductance from the measurements:

$$M = \left(\frac{.0928}{9.889}\right)\frac{49.9}{2\pi(500100)} = 1.49e-7 \text{ Henries}$$

The percent error between expected and measured is

(1.58-1.49)/1.58*100=5.7%

Which is not bad; however, if you study the oscilloscope trace, you will notice high-frequency "saw-tooth" wave riding on the output wave (CYAN). This is a problem indicative of the digital synthesis of the source wave. The discrete jumps in the source wave (not noticeable unless the source wave is magnified), represent very high frequency (at least 20X) changes that transfer to the output loop with a much higher degree of efficiency than the fundamental frequency of the source. This error in the output trace obscures the accuracy of the result.

We can eliminate this problem by switching to a function generator which does not use digital synthesis. Figure 8-11 shows a scope screen capture of the test conducted with the analog function generator. Because our analog function generator does not have the frequency or power output of the digital unit, we have a much smaller output signal. In any case, you will notice that the output signal (CH2: CYAN) is much cleaner.

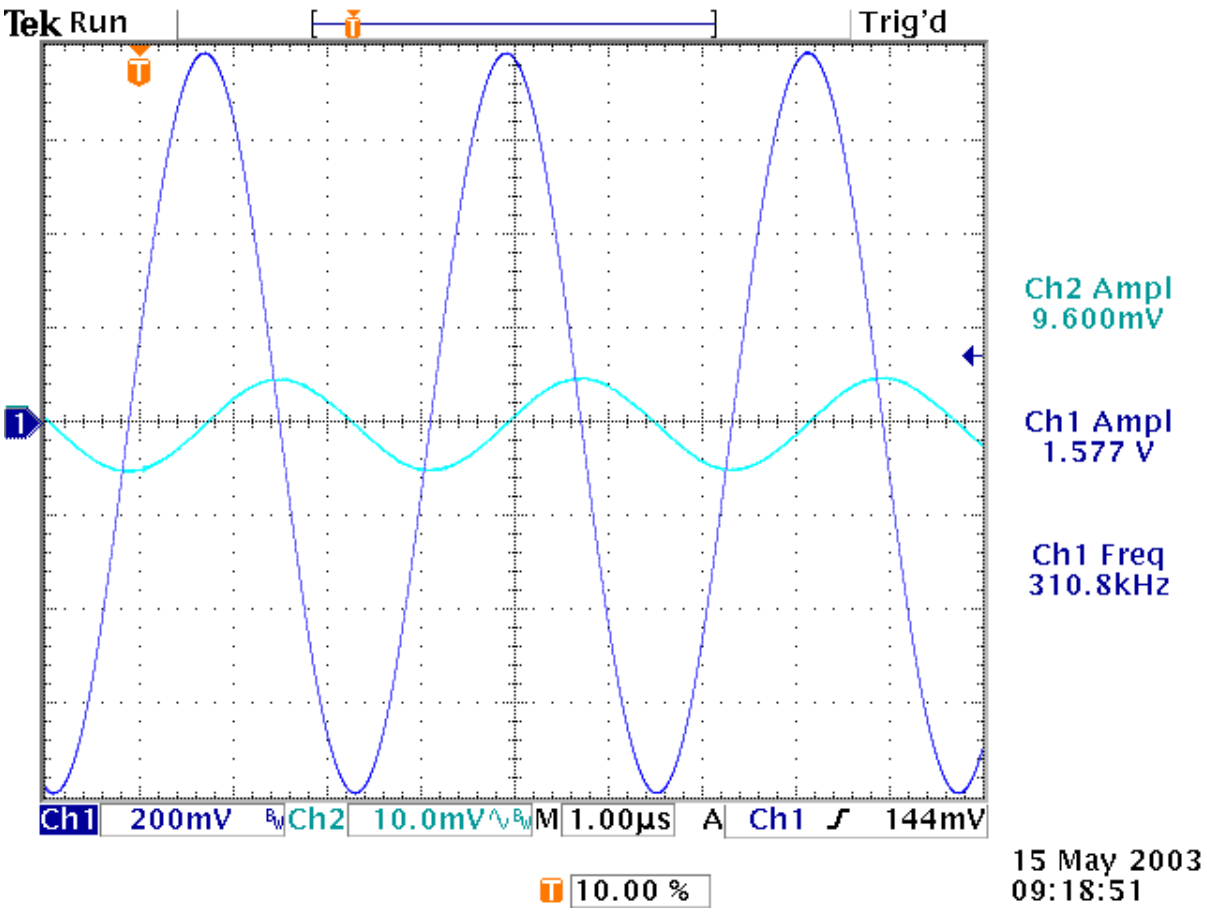

Figure 8-11 Using JDR instruments DOS-600 Audio function generator (analog)

To calculate the mutual inductance from the
Applying the relationship from step 11:

$$M = \left(\frac{.0096}{1.577}\right)\frac{49.9}{2\pi(310800)} = 1.56e-7 \text{ Henries}$$

The percent error between expected and measured is
(1.58-1.56)/1.58*100=1.3%

The remaining error in the measurements is most likely a combination of the harmonic distortion of the function generator and the inaccuracies in construction. For paper and glue construction, 98% accuracy is respectable.

For fun, try calculating the emf of this loop using Faraday's Law.

9 Parasitic loops

Add a closed loop to the previous example and label it O (for other). Again, like the previous example, we drive the source loop with a time changing current and would like to know the kinetic voltage (emf) developed in the target; however, in this example we would like to know the effect of the other (or parasitic) loop on the amount of energy that is coupled to the target.

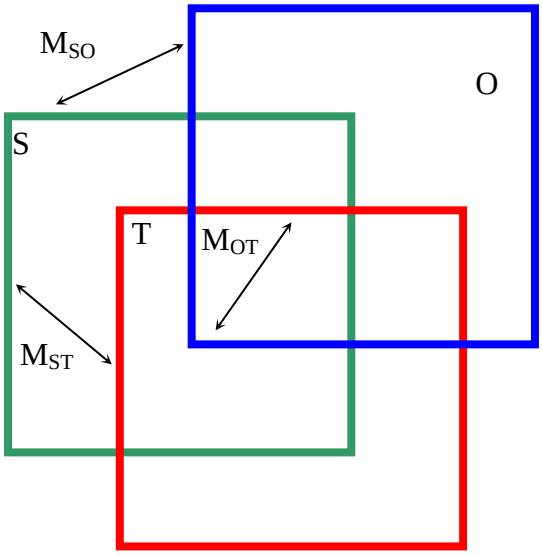

Figure 9-1 Parasitic loop example

Using New Inductance, it is quite easy to determine the mutual couplings (M_{OT}, M_{SO}, M_{ST}) between the loops. In this example, we use rectangular loops since we provide an algorithm for calculating the couplings between rectangular loops with this book (See NIA1.xls).

Note: M_{OT}, M_{SO} and M_{ST} are DC mutual inductive couplings as defined in section 4.2.2

The following are also introduced
L_O=inductance of the O loop
R_O=resistance of the O loop

We seek to know the kinetic voltage (emf) induced in the target trace resulting from changes in current through the source. The total kinetic voltage is the sum of the direct and indirect (or reflected) energy. The direct energy is coupled

from source to target and the indirect energy is coupled from current changes induced in the O loop. The current changes in O are induced from current changes in the source.

Let us begin by deriving an expression for the indirect (or reflected) coupling. To do this we start by determining the kinetic voltage coupled to the O loop:

1) $V_{KO} = -M_{SO}\frac{di_S}{dt}$

The following diagram shows that the kinetic voltage induced in a circuit is opposed by potential voltages arising from "voltage drops" across the loop parameters. Note: The following picture is generic and therefore does not show the "O" subscripts.

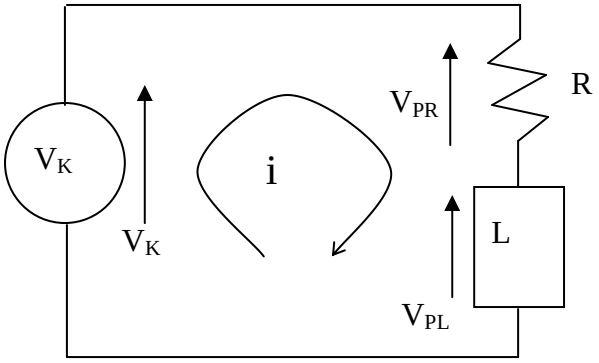

Figure 9-2 Relation between kinetic and potential voltages in a loop

Using the concepts demonstrated in the above picture, we write the sum of the potential voltages ("Voltage drops") in the outer loop as:

2) $V_{PO} = -i_O R_O - L_O\frac{di_O}{dt}$

The New Electromagnetic form of Kirchhoff's Law is: The sum of the kinetic voltages around the loop plus the potential voltages must equal zero or

$0 = \sum V_K + \sum V_P$ (for closed loops only)

In our case above:

3) $0 = V_{KO} + V_{PO} = -M_{SO}\frac{di_S}{dt} - i_O R_O - L_O\frac{di_O}{dt}$

The next step is to derive the current in O as a function of the current in the source loop. The easiest way to do this is to Laplace transform step 3:

4) $0 = M_{SO}SI_S(s) + I_O(s)R_O + L_O SI_O(s)$

Then solve for I_O:

5) $I_O(s) = -\frac{M_{SO}SI_S(s)}{R_O + L_O S}$

Now that we have an expression for the current in O, we can then find the total kinetic voltage induced in the target by summing the coupling of the effects in the source and outer loops as such:

6) $V_{KT} = -M_{ST}\frac{di_S}{dt} - M_{OT}\frac{di_O}{dt}$

Transform step 6:

7) $V_{KT}(s) = -M_{ST}SI_S(s) - M_{OT}SI_O(s)$

Substituting step 5 into 7 yields

8) $V_{KT}(s) = -M_{ST}SI_S(s) + M_{OT}S\frac{M_{SO}SI_S(s)}{R_O + L_O S}$

Rearranging

9) $V_{KT}(s) = -\left[M_{ST} - \frac{M_{OT}M_{SO}S}{R_O + L_O S}\right]SI_S(s)$

Thus the total EXACT mutual coupling between source and target with the effects of the parasitic (O) loop is:

$$M_{TOTAL} = M_{ST} - \frac{M_{OT} M_{SO} S}{R_O + L_O S}$$

Equation 9-1: Total Coupling

The quantity $(-\frac{M_{OT} M_{SO} S}{R_O + L_O S})$ in the above equation is the "reflected" coupling resulting for the existence of the parasitic loop.

$$M_{REFLECTED} = -\frac{M_{OT} M_{SO} S}{R_O + L_O S}$$

Equation 9-2: Reflected Coupling

If the frequency of operation is such that $R_O << \omega L_O$, then the above reduces to

$$M_{REFLECTED} = -\frac{M_{OT} M_{SO}}{L_O}$$

Equation 9-3: Simplified Reflected Coupling

The reflected coupling has some very interesting properties:

1) It is a high pass characteristic.
2) Below the break frequency, most energy in the O loop is absorbed by the resistance of the loop; therefore, below the break frequency is more optimal for induction heating.
3) Above the break frequency, most of the energy in the O loop is re-emitted into space; therefore, above the break frequency is optimal for operation as a parasitic loop (for sensor and radio applications).
4) Above the break frequency, the reflected energy is 180 degrees out of phase with the incident energy.

Section 15.3.4 validates the derivation in this section by comparing the measured and calculated coupling between three loops (S, T and O).

Application 1: Smart Metal Detector

A metal detector can be made in which the parasitic loop is a gold ring or a coin buried in the sand. By using frequency scanning techniques and multiple sets of source and target and loops, such a metal detector could determine the orientation and depth of conductive objects. With even more sophistication

(phased array techniques) it should be possible to produce a 3-d image of the buried object and be able to determine the type of material.

Application 2: Wireless Solid State Multiple Axes Position Sensing

In classical applications of electromagnetic position sensing, the direct coupling between a source loop(s) and target loop(s) is used as the means to determine the position of an object. This requires wires to be attached to the object whose position is being measured.

Using the techniques shown in this section, it becomes possible to place a parasitic loop in the moving object and detecting its position from a stationary array of detectors and at least one emitter.

10 Conductive Planes

10.1 Single Conductive Plane

A conductive fragment containing a time changing current is suspended over an infinite, perfectly conductive plane. The inductive effects from the source fragment induce surface currents in the conductive plane. These surface currents generate an inductive field effect that is equivalent to a NEGATIVE image of the source as shown in Figure 10-1. This is the New Induction equivalent of the classical technique known as "The Method of Images" (MOI for short).

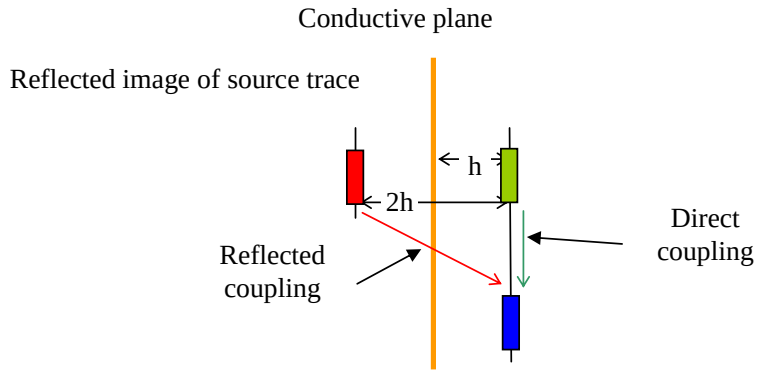

Figure 10-1 Method of Images for single conductive plane

Referring to the above diagram, a target fragment (blue) experiences the combined inductive effect of the source and the negative image that appears in the conductive plane as given by the following expression:

$M_{TOTAL}=M_{DIRECT}-M_{REFLECTED}$

The complete derivation of this "Method of Images" (MOI) for induction is contained in another book in the New Electromagnetism Application Series. The derivation shows that the thickness of the conductive plane along with material properties affects the efficiency of reflection. For standard 1 oz. copper PCB conductive planes, we use 97% as an approximation for the reflection efficiency ($\eta = 97\%$). Adjusting the above relationship to account for the reflection efficiency yields:

$$M_{TOTAL} = M_{DIRECT} - \eta M_{REFLECTED}$$

If you did not follow the above description, it will become clear when it is applied in later section.

10.2 Parallel Conductive Planes

The reflection from two parallel conductive planes is a bit more complicated. This is highlighted by remembering what happens when you stand between two parallel mirrors, you notice that there are infinite copies of yourself windowing out toward infinity. Figure 10-2 shows the reflections cast from a light bulb between two parallel mirrors.

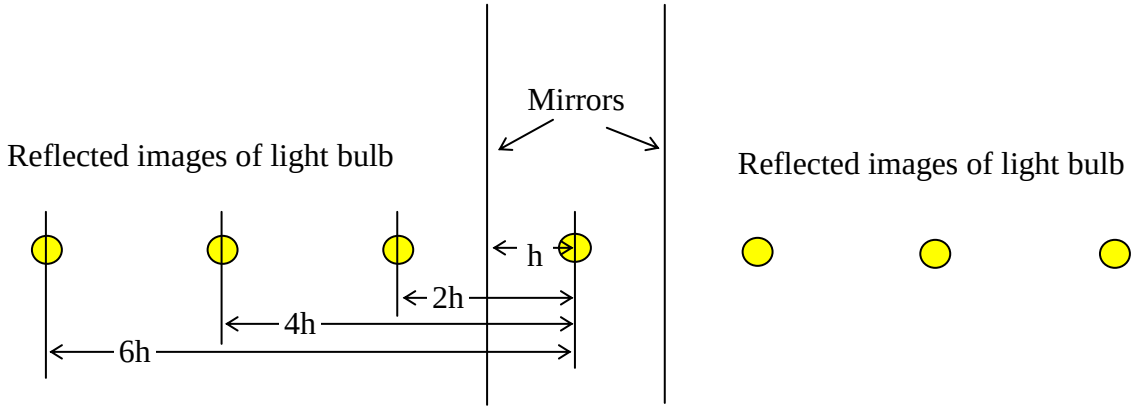

Figure 10-2 Light bulb between mirrors

When determining the reflections of a source loop between two conductive planes, we utilize the same pattern of reflections except that every other reflection is positive instead of negative as shown in the next figure.

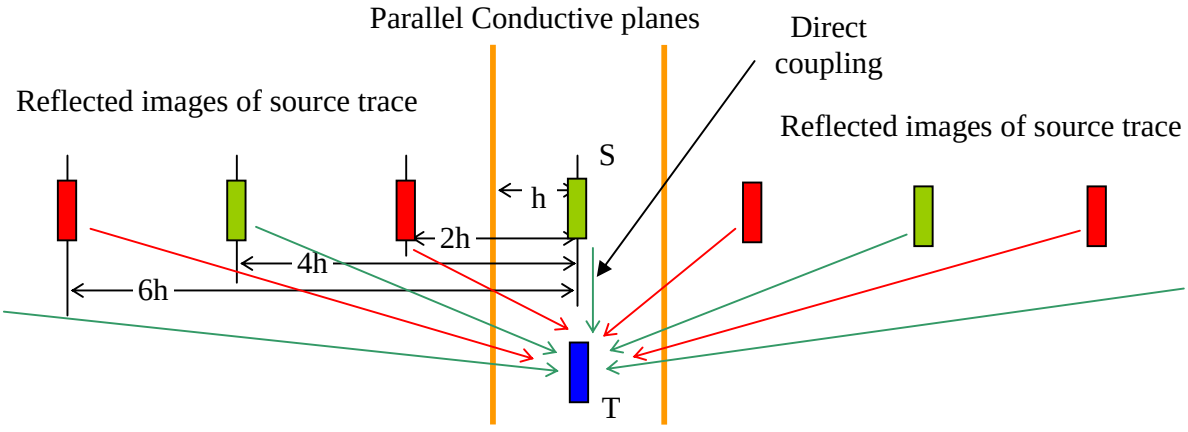

Figure 10-3 Inductive reflections from conductive planes

For a simplified case where the conductive material reflects with 100% efficiency we simply sum the following couplings

$M_{TOTAL}=M_{DIRECT}-2M_{2h}+2M_{4h}-2M_{6H}+\ldots$

Since copper is not a perfectly reflecting material we assign it a coefficient of reflection $\eta = 97\%$.

Since the 2h images are the result of one reflection, and the 4h are the result of 2 reflections, etc. Then the above relations is modified for "real world" conductive surfaces as follows

$$M_{TOTAL} = M_{DIRECT} - 2\eta^1 M_{2h} + 2\eta^2 M_{4h} - 2\eta^3 M_{6h} + 2\eta^4 M_{8h} \ldots$$

All of the Ms in the above equation can be calculated for parallel or rectangular loops using the derivation from the previous sections or the included software. An example (with experimental evidence) of a mutually conducting system with the effects of parallel conductive planes is found in section 15.3.3.

Using the New Induction model, the reader can derived the general solution for any given type of wire system.

11 PCB / IC Trace Cross-Talk

Each year, printed circuits boards (PCB) and integrated circuits (IC) become smaller and smaller, forcing signal paths closer together to allow for higher densities and frequencies of operation. The drawback to this progress is that the electromagnetic coupling between these signal-paths (traces) increases dramatically. The electromagnetic coupling causes signal energy from one trace to "bleed" into, and interfere with, the signal on another trace causing what engineers call cross-talk.

The electromagnetic coupling between traces (cross-talk) is caused by both capacitive and inductive coupling. This section focuses on the cross-talk resulting from inductive coupling.

This application considers the case where the source trace (the one emitting the energy) and the target trace (the one experiencing the cross talk) do not have any conductive traces between them (interstitial traces). The absence of interstitial traces represents the worst case scenario since interstitial traces will most likely mitigate cross-talk effects unless the interstitial trace happens to have a high-Q resonant behavior; in which case, Q-Rise may cause problems.

11.1 Single Conductive Plane

The first example considers the cross talk (inductive) between two traces suspended over a single conductive plane.

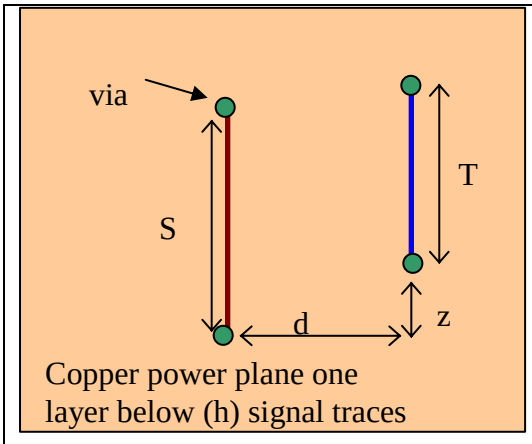

Figure 11-1 Top View of Example

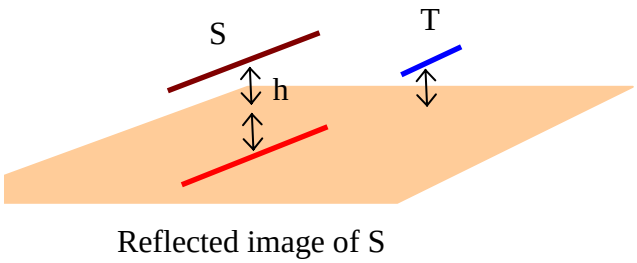

Figure 11-2 Oblique View of Example

The source and target trace are suspended over a ground plane at distance h (Figure 11-1,Figure 11-2). In the figure, the two traces originate and end on other signal planes; in this example we are only looking for the effect on the north-south routing plane where these sections of the signal paths co-exist.

The first step is to determine the effect of the source on the target. This is done by calculating the parameters required for the Parallel Filament equation. These parameters are determined as follows:

Algorithm Parameter	Use
S	S
T	T
D	d
P	T/2+z-S/2

These parameters are then inserted into the algorithm to get the first component of cross talk M_{DIRECT}.

Next we need to determine the effect of the conductive plane. In section 10.1 we discussed the reflective behavior of inductive elements with respect to conductive planes. From this understanding, the reflected effects are calculated as if a negative image of the source exists below the conductive plane (see Figure 11-2). The effect of the reflected image is calculated from the following parameters

Algorithm Parameter	Use
S	S
T	T
D	sqrt(d*d+h*h)
P	T/2+z-S/2

These parameters are then inserted into the Parallel Transverse filament algorithm to determine the reflected coupling $M_{REFLECTED}$.

Since the reflected effects are negative, the total inductive coupling between source and target is

$M_{TOTAL} = M_{DIRECT} - \eta M_{REFLECTED}$

A complete example of the effect of ground plane on PCB cross talk is calculated and verified by experiment in section 15.3.2.

11.2 Double Conductive Planes

If the source and target were sandwiched between two conductive planes, the coupling becomes vastly more complex as shown in section 10.2.

A worked out example of the effect of two conductive planes (which includes experimental verification) is found in section 15.3.3. Needless to say, two conductive planes reduce the coupling between signal traces better than a single plane.

11.3 Conclusion

The above results show that the reflected coupling from conductive plane(s) reduces the total cross talk received by the target trace.

The calculated results in section 15 use 97% as an approximation for the reflective efficiency.

These derivations also assume that the conductive planes are solid (no pattern).

The conductive planes not only mitigate cross-talk they also help reduce trace inductance as demonstrated in the transmission line section (section 14).

The techniques shown in this section can be expanded to account for all effects as desired. www.distinti.com is producing PC compatible software that will allow complete analysis of trace cross-talk (both inductive and capacitive) from Gerber type files.

12 PCB / IC Transformers

With the technology revealed in this book it becomes possible to design PCB/IC traces in such a manner to intentionally provide coupling between circuits; effectively using the PCB/IC artwork to provide for small high frequency transformers.

In section 15.3.1 such a transformer is realized. The rectangular loops software predicts that the coupling between the primary and secondary is 125nH and the experimental results show 123nH.

Note: you can use any shaped loop you desire; we are using rectangular loops in this example since rectangular loops are provided for in the software which accompanies this book.

Naturally the effects of conductive planes and parasitic traces need to be accounted for. These effects are all considered in other sections.

A drawback to PCB/IC transformers is that they are typically low-Q transformers which should not be used for power applications.

Our Software Package GEM3 will enable you to specify PCB or IC transformers based on many factors to include frequency response, Q, and a number of other considerations.

13 EMI Considerations

The high frequency signals from PCBs or ICs readily emit inductive energy into space (as demonstrated in previous sections). This inductive energy can couple to other circuits in either beneficial or harmful ways. Examples of beneficial couplings include wireless communication, PCB transformers, trace impedance reductions (next section) and inductors. Harmful couplings include cross-talk, and electromagnetic interference (EMI) which disrupts broadcast communications.

It's a common practice to provide a conductive shield to prevent EMI emission and/or reception. The effectiveness of the shield depends upon the configuration of the shield.

Section 9 discusses the effects of solid conductive planes between the routing layers in PCBs. The conductive planes reflect and refract the inductive energy emitted by signal traces. The reflected or refracted energy results from eddy currents induced in the plane from signal traces. The ratio between reflected and refracted energy depends upon the conductivity of the shielding material. As the material approaches perfect conductivity (such as a super conductor) all of the energy is reflected back with 180 degree phase shift. This reflected energy can couple back to the original circuit causing either harmful or beneficial effects. The manner in which a perfect conductor prevents radiation from passing through is shown in the following diagram. The green trace is the source signal which travels to the right. The source signal induces currents in the surface of the shield which emit a negative signal in all directions from the incident point (see red trace).

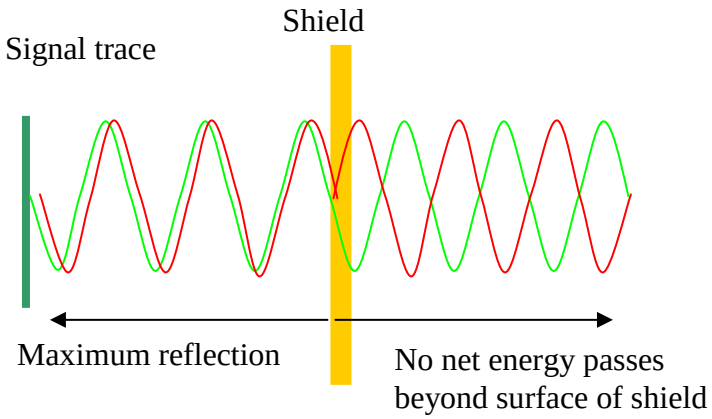

Figure 13-1 A perfectly conductive shield

This induced signal on the right combines with the original source signal to cancel all energy to the right of the shield surface. The induced signal on the left (green) is effectively the reflected source signal.

If a different shield material were used that had a conductivity which approaches zero, no eddy currents are induced. As such, the energy passes completely through the shield. Note: this does not apply to certain magnetic materials, a complete accounting of magnetic materials to be released in New Magnetism Applications: Volume 2 (NMA2) which is another book in the New Electromagnetism Application Series.

In most cases, shields are made of some material with properties between a superconductor and an insulator. The following figure shows the shield material constructed from a "good" conductor.

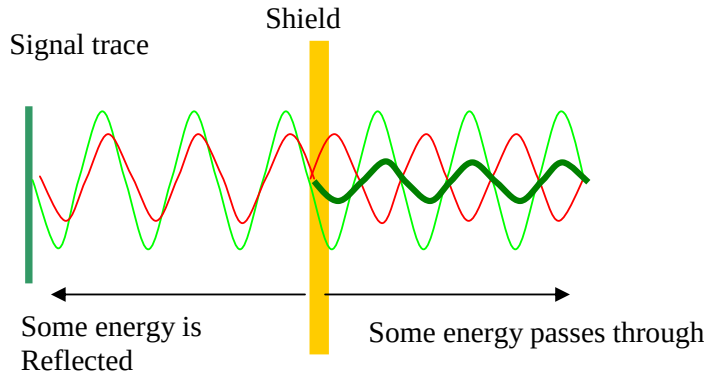

Figure 13-2 A good conductor

Because the material is not perfectly conductive, the incident wave is unable to induce a complete and opposite affect in the first few layers. In fact, because the incident wave is not outright cancelled, the inductive effect is able to affect charges deeper into the conductive material. Each layer that is affected provides a certain amount of cancellation until the remainder of the signal passes out the other side (shown above). If the material were thick enough, the signal energy would be completely prevented from passing through.

The above considerations open up a new branch of electromagnetic physics that we call inductive reflectometry and refractometry. This new science is released in detail in the book NIA3 (New Induction Application Series: Volume 3: Inductive Reflectometry and Refractometry). NIA3 has applications raging from EMI control to remote material identification to Stealth technology.

14 Transmission Lines

Any arrangement of conductors that transmits a signal from one place to another is considered a transmission line. Unlike Antennae modeling, all of the electromagnetic effects must be accounted for in order to develop a complete model for the behavior of such systems.

The following diagrams show the two types of transmission lines that are considered in this section.

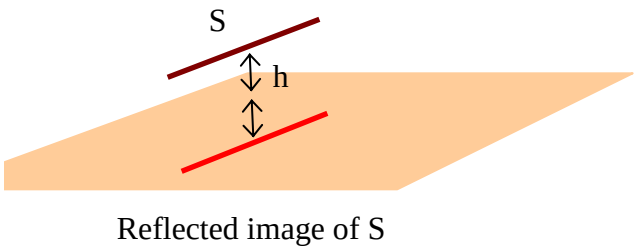

Figure 14-1 Single wire over ground plane

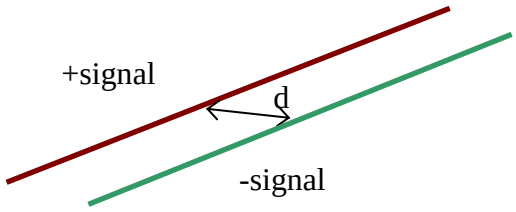

Figure 14-2 Two wire

A strait length of conductive conduit, by itself, has a measurable inductance that is comprised of two components. The first component is the self-inductance and the second is the intrinsic-inductance. These two components combine to give the inductance L_C of the conduit by itself. L_C is a function of wire thickness, cross sectional shape, length and the properties of the conductive materials. L_C is discussed in great detail in another text in this series which covers intrinsic and self inductance in great detail. For this text, L_C is a given quantity.

For simplicity, these derivations assume that the signal wave length is much longer than the signal path. This allows use of simple lumped parameter analysis. For the case where the transmission line is longer than the signal wave length, our GEM3 software package will be able to determine the transmission line characteristics.

14.1 Wire over ground plane (PCB/IC)

The wire over ground plane transmission line is commonly used in printed circuit boards and integrated circuits.

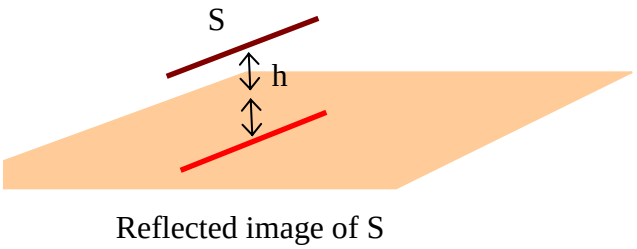

Figure 14-3 Microstrip

Other sections of this text discuss how the energy reflected from the ground plane actually serves to minimize cross-talk interference between traces (see section 9). This section will show how energy reflected from the ground plane minimizes trace impedance.

As stated, the signal conduit, by itself, has an inductance that we have assigned the quantity L_C. Using the MOI, the energy reflected from the conductive plane couples energy back to the source that helps to mitigate this inductance. Using the Parallel Transverse Filament equation, we insert the following quantities to determine the amount of reflected coupling ($M_{Reflected}$)

Algorithm Parameter	Use
S	S
T	S
d	2h

The total inductance of the transmission line is the difference between L_C and $M_{REFLECTED}$ or

$L_{TOTAL} = L_C - \eta M_{REFLECTED}$.

The above relationship is verified in section 15.3.5

If the height of the conduit is lowered, the total inductance of the conduit diminishes; however, the capacitive coupling (C) between the conduit and conductive plane increases drastically.

The model of the transmission line then becomes:

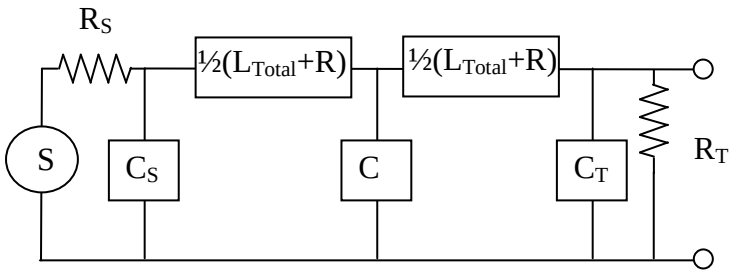

Figure 14-4

In the Above diagram, C_S is the total capacitance of the Source output and soldering pad. C_T is the total capacitance of the termination device input and soldering pad. R is the resistance of the conduit.

Note: The above model does not account for leakage between the signal path and ground because this is a short transmission line (under 20cm). We only demonstrate how the reflected image of the line affects the inductance of the line with respect to transmission line modeling. You are free to apply these inductive effects to whatever transmission model you desire.

For a high frequency version of this transmission line it is converted into a distributed parameter model as shown in Figure 14-5. Accuracy increases as n increases. For best results, n should be more than 4 times the number of waves that fit in the line; preferably greater than 16 times.

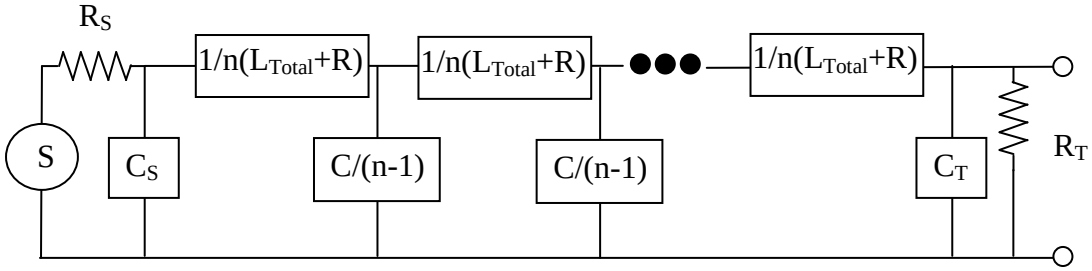

Figure 14-5 Distributed parameter version of the transmission line

Depending upon your application, other loss parameters may need to be considered.

This text shows how inductive effects from the ground plane affect the transmission line model. These effects are not properly addresses in classical texts (except by empirical means) since classical electromagnetic field theory does not allow direct analysis of these effects.

14.2 Twin Parallel Wire

In a twin wire transmission system, a signal and its negative are sent through the transmission line simultaneously.

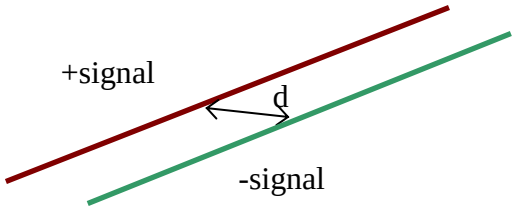

Figure 14-6

As in the previous example, each conduit possesses an inductance that we assign the value L_C.

Since New Induction teaches us that two parallel wires couple electromagnetically, we have another inductive component due to the mutual induction between the two conduits.

The mutual induction between the two conduits (M) can be determined using the Parallel Transverse Filament algorithm by inserting the following parameters

Algorithm Parameter	Use
S	Length of TX line
T	Length of TX line
d	d from diagram

The low frequency model of the transmission line is

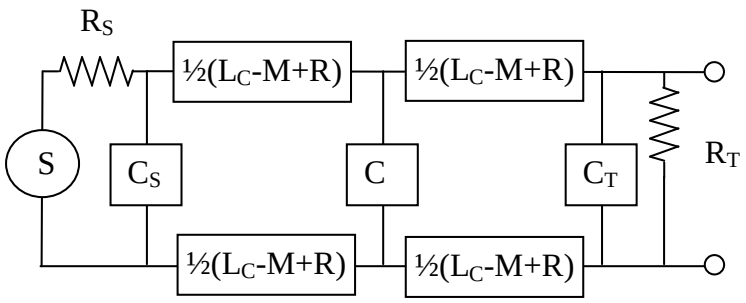

Figure 14-7 Low frequency approximation (for diametric signals)

Note1: the above assumes that equal and opposite signals (diametric) are sent.

Note2: The above model does not account for leakage between the two signal paths (required for long transmission lines). We only demonstrate how the cross coupling between the two lines affect the inductance of the system. You are free to apply these inductive effects to whatever transmission model you desire.

For high frequency approximation, techniques similar to the previous section may be employed.

For a two wire transmission line where it is desired to send independent signals (asymmetric) through each wire, or there are multiple conduits in a bundle where it is desired to model the cross coupling, the following circuit approximation is used:

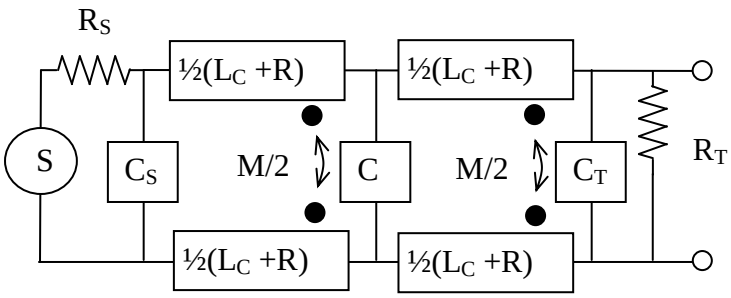

Figure 14-8 For Asymmetric signaling

In the above circuit, the two conduits are coupled like transformers where a current increase in one wire induces a kinetic voltage (emf) in the opposite direction in the other wire (The dot notation shown is correct). For best results, n should be more than 4 times the number of waves that fit in the line; preferably greater than 16 times.

15 Experimental Validation

In many chapters of this book, we develop theoretical applications of New Induction which highlight the exact nature to which mutual and reflected couplings can be derived from New Induction. In this section, we use a versatile device called an inductance template to verify the theoretical predictions of the previous chapters.

15.1 The Inductance Template

Figure 15-1 shows an inductance template. It is a single sided PCB etched with conductive constructs that enable us to validate the theoretical observations made in the previous sections.

In this book, we only use a few of the square loops shown in the lower left of the template. The remainder of this board is used to verify self-inductance and intrinsic-inductance models derived in NIA2.

The inductance template is constructed from 1/16 inch single sided PCB board with 1oz copper. Also used (but not shown) are two more single sided copper PCBs (of 1oz copper; un-etched) which are used to measure the effects of conductive planes.

In this section we use the four outermost square loops shown on the lower left side of the template. These loops are 20mils thick and 50 mils center to center.

Figure 15-1 Inductance template

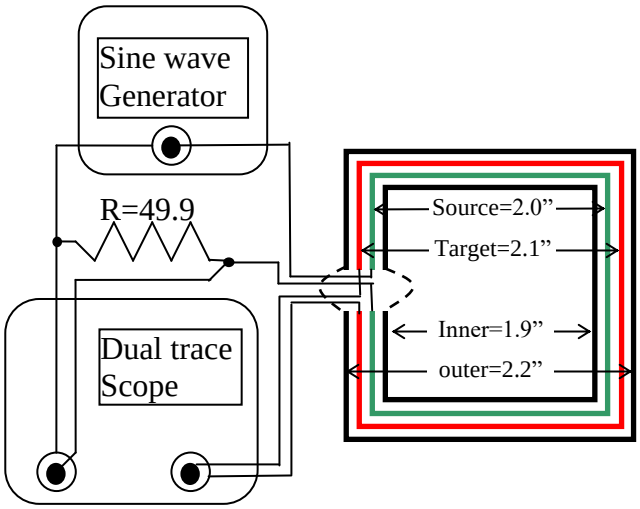

Figure 15-2 Inductance template circuit

The outer and inner loops are selectively closed or open for each test. The inner and outer loops allow us to calculate the effects of parasitic loops. For certain

test, the inductance template is sandwiched between a top and bottom conductive planes to measure the effects of conductive layers.

Figure 15-3 Inductance template sandwich

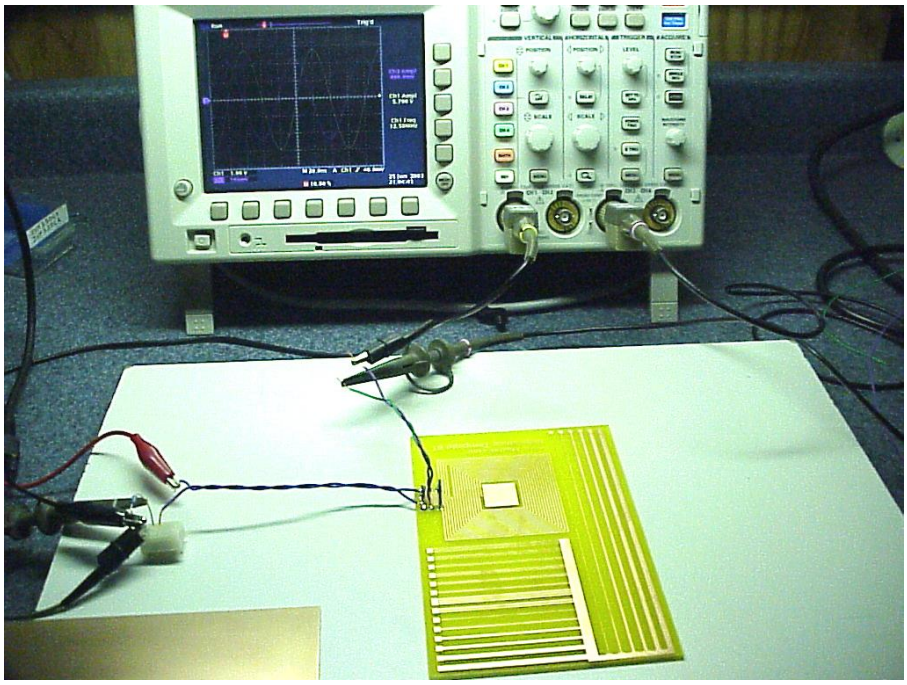

Figure 15-4 The inductance template connected to scope and function generator

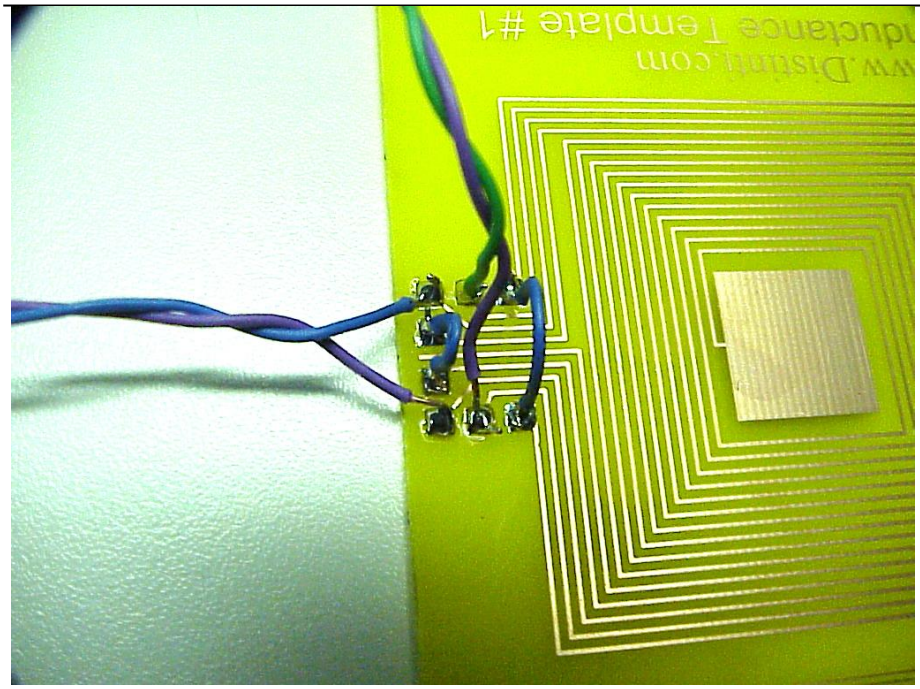

Figure 15-5 Close up of soldered connections to template (no conductive planes shown)

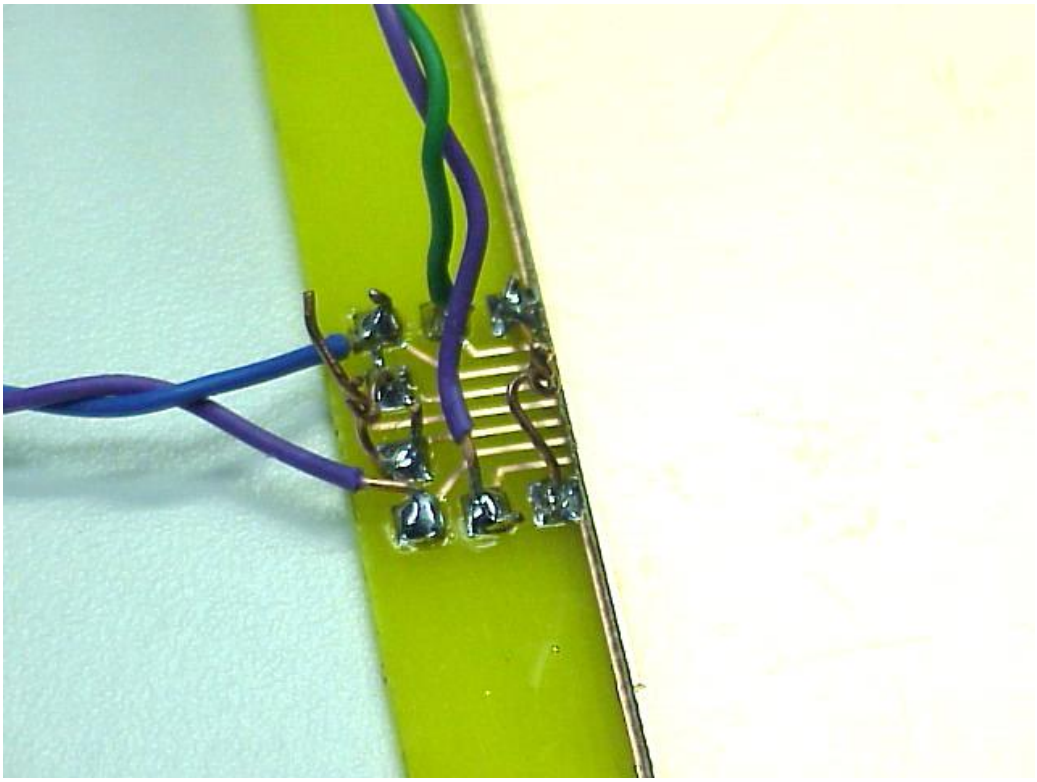

Figure 15-6 When conductive planes are used, they will not cover traces beyond the outermost loop

The following table outlines the measurements of the Inductance template with conversions to meters for use with the software.

Measurement	Symbol	English	Meters
Inner	I	1.9”	0.04826
Source	S	2.0”	0.0508
Target	T	2.1”	0.05334
Outer	O	2.2”	0.05588
Board thickness	B	58mils=0.058” (this is measured)	0.0014732
Copper thickness	C	1oz	0.000035
Distance between layers	h=B+C		0.0015082
Distance between loops	d	50mils	0.00127

15.2 Measured Couplings

The ability to measure inductive couplings accurately requires minimization of capacitive coupling. One of the best methods is to drive the source loop from a current source. The following section details a simple single transistor circuit that will give reasonable good results.

15.2.1 Standard circuit

The standard circuit used for measuring mutual and reflected couplings (Figure 15-4) was used with a signal frequency of 12.5MHz. Because the source loop electrically bounces from positive to negative, there is capacitive coupling between source and the target loop which interferes with the measurements causes the values to be too high. The interference is not really that bad; however, we opted to use a transistor current source (next section) to reduce the voltage swing of the source to reduce the error caused by capacitive effects.

The 12.5 megahertz results are included in the web support pages (see back cover).

15.2.2 Simple transistor current source

In order to reduce the capacitive coupling between the source and the target, we drive the source loop with a current source which minimizes (it doesn't eliminate) the voltage swing of the source. The following diagram shows the circuit diagram. The diagram also shows the source and target loops of the inductance template.

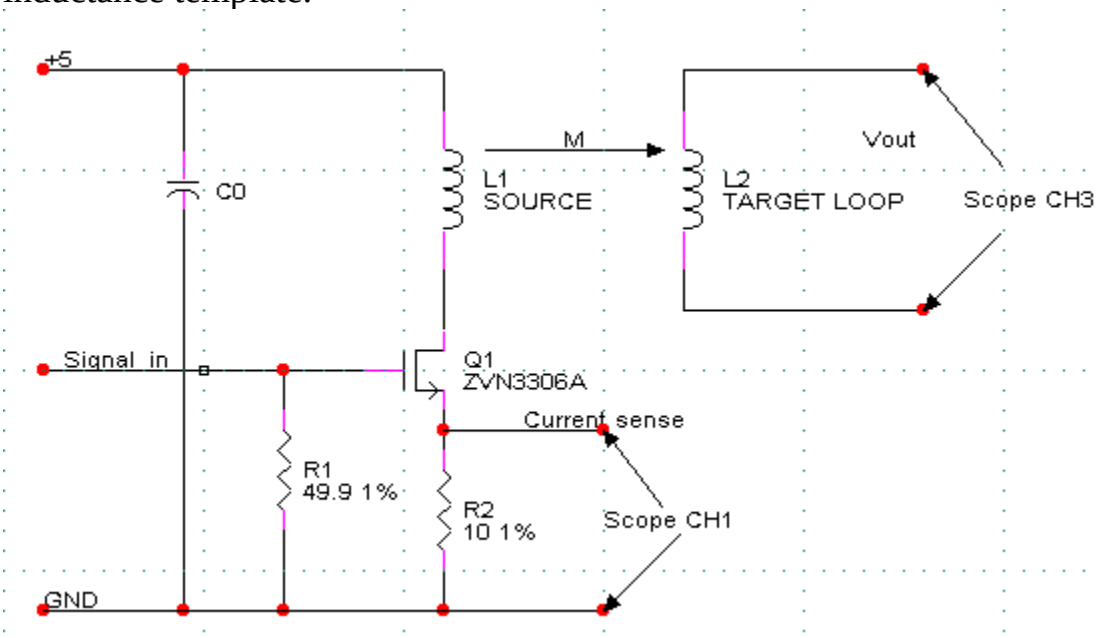

Figure 15-7 The single transistor current source

Note: C0 in the diagram above is the combined capacitance of many capacitors as shown in the following photographs. Enough capacitance should be used to reasonably smooth the deflection of the power supply caused by this circuit. Use large radial electrolytic (low ESR) combined with medium tantalum and some high frequency monolithic and mica capacitors for good measure.

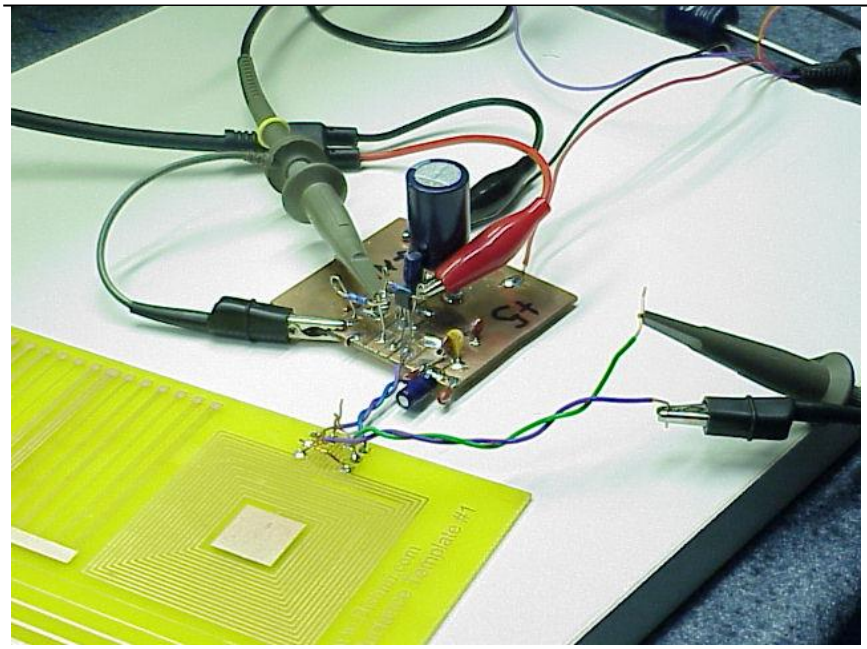

Figure 15-8 The single transistor current source coupled to Inductance Template

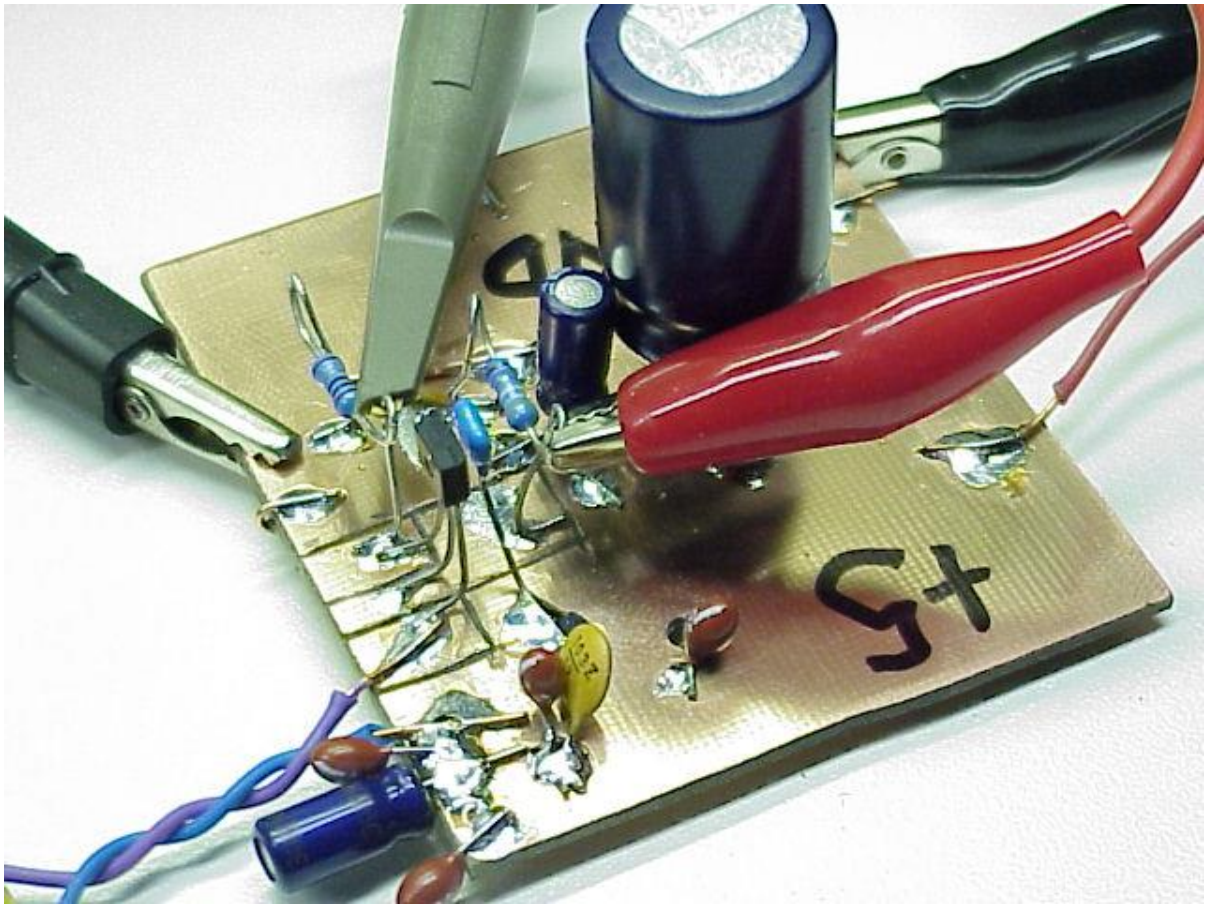

Figure 15-9 Blow up of circuit; back side of circuit board is solid ground plane

The key to operating this circuit is to find a suitable operating point for the transistor. We found a suitable operating point by setting our function generator (Tektronix AFG310) to sine wave 0.8V amplitude (peak-peak) and 3.2Volt offset.

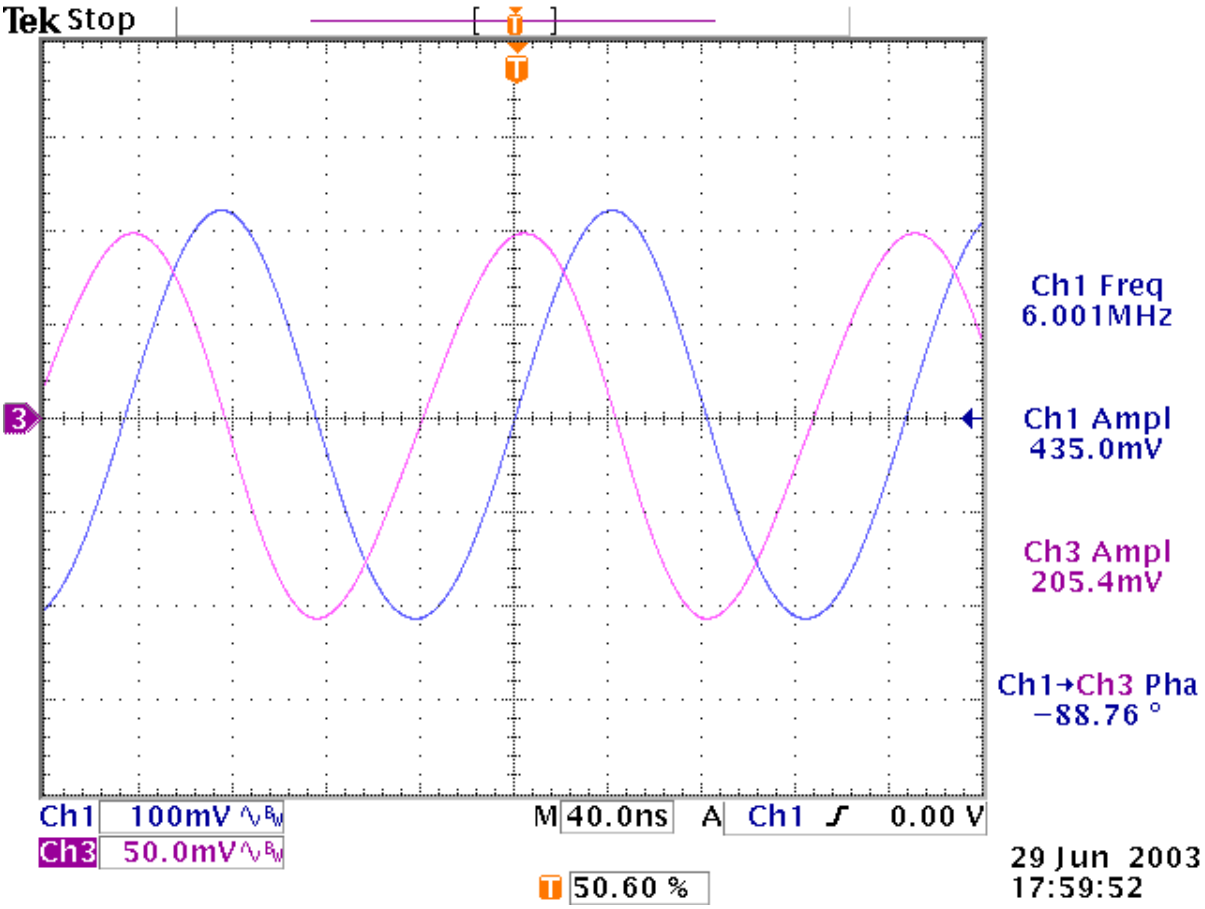

Figure 15-10 measurement of template with no conductive planes or parasitic loops

The above scope screen capture shows some distortion (bottom halves of CH1 sine waves are slightly wider than top halves); however, the distortion does not throw measured values off too much since the wave received from the target loop (CH3) has similar distortion (tops are wider).

Table 2: Inductance Template Tests

Inductance Template tests 6 Mhz Tests

Measured

test	lower	upper	inner	outer	s	t		freq	Vs	Vt	R	M(nH)
1	0	0	0	0	2	2.1		6	435.0	205.4	10	125.25
2	1	0	0	0	2	2.1		6	434.4	68.0	10	41.52
3	1	1	0	0	2	2.1		6	434.5	43.6	10	26.62
4	0	1	0	0	2	2.1		6	434.5	69.2	10	42.25
5	0	0	1	0	2	2.1		6	436.8	124.8	10	75.79
6	1	0	1	0	2	2.1		6	434.3	59.7	10	36.44
7	1	1	1	0	2	2.1		6	432.0	41.2	10	25.30
8	0	1	1	0	2	2.1		6	434.4	60.9	10	37.19
9	0	0	1	1	2	2.1		6	434.2	83.7	10	51.12
10	1	0	1	1	2	2.1		6	432.0	52.6	10	32.30
11	1	1	1	1	2	2.1		6	432.0	38.9	10	23.88
12	0	1	1	1	2	2.1		6	434.5	53.4	10	32.60
13	0	0	0	1	2	2.1		6	434.8	120.4	10	73.45
14	1	0	0	1	2	2.1		6	434.9	60.0	10	36.60
15	1	1	0	1	2	2.1		6	434.2	41.2	10	25.17
16	0	1	0	1	2	2.1		6	434.6	61.0	10	37.23

In the above table, the columns “lower” and “upper” are set to one if the test was performed with lower or upper conductive planes (respectively). The columns “inner” and “outer” are set to one when the inner or outer loops (respectively) are closed.

15.2.3 Other Data

Other measured data is the trace inductances and trace resistances.

Trace resistances

We used the DVMx1000 to measure the very low resistances of the traces. This procedure is shown in the DVMX1000 user’s manual which is free for download from our site.

The resistances are

- Inner= 0.294 Ohms
- Source = not measured: interpolated at (308-294)*1/3+294=299
- Target =not measured: interpolated at (308-294)*2/3+294=303
- Outer =0.308 Ohms

Trace Inductance of Outer Loop

We used our proprietary Nanoinductance meter to measure the trace inductance of the outer loop for comparison to calculations regarding trace impedance

Outer loop trace inductance

- 260 nH with no conductive planes
- 169 nH with bottom conductive plane
- 153 nH with top and bottom plane

15.3 Calculated Couplings

In the following sections, the various tests of the Inductance Template (found in Table 2) are calculated from the theory presented in other sections of this book. The calculated results are then compared to the results fromTable 2. By comparing theoretical to experimental results, this section validates the theories presented in this book.

15.3.1 The primary to secondary (Direct) coupling

This is the mutual inductance between the source and target loops with the inner and outer loops open and no conductive planes.

For this calculation, we use the following parameters in the Rectangular loops algorithm

Algorithm Parameter	Use
LX1,LY1	S=0.0508
LX2,LY2	T=0.05334
PX2,PY2	-d=-0.00127
PZ2	0
N1,N2	1
Result	123 nH

The measured value from Table 2 line 1 is 125nH. There is excellent agreement between experimental and theoretical results.

15.3.2 Coupling with single conductive plane

Using the theory in section 10.1 we calculate the total coupling between a source and target trace with the added effect of a ground plane.

The direct coupling is the same as in section 15.3.1.

To calculate the reflected image of the primary (as observed by secondary), the following parameters are entered

Algorithm Parameter	Use
LX1,LY1	S=0.0508
LX2,LY2	T=0.05334
PX2,PY2	-d=-0.00127
PZ2	2*(0.0015082)=0.0030164 The reason why this is multiplied by two is that the reflected image is twice as far as the conductive plane.
N1,N2	1
Result	85.4 nH

Because the copper is not perfectly reflective, we multiply the result in the above table by the reflection coefficient (97% is the approximation that we use throughout this book. Exact coefficients for many materials are released in another book in this series).

Calculating the total mutual inductive linkage between primary and secondary with one reflecting copper plane:

123nH – 85.4*0.97 = 40.2nH

The measured values are:
42.25nH with upper plane only
41.52nH with lower plane only

There is excellent agreement (within 5%) between theoretical and experimental.

Note: the reason for the difference between the upper and lower measurements is due to the fact that the upper conductive plane was slightly farther away from the source and target than the lower plane. The difference in distance was

measured to be about 30 microns. This correlates to PZ2=0.0030764 which yields -84.8 nH. Thus 123-84.8(.97) = 40.74nH.

15.3.3 Coupling with two conductive planes

To find the coupling between the source and target loop with two conducting planes, we use the theory presented in section 10.2.

We sum the following Couplings:

Coupling	Calculated value	Corrected value	Reflection coefficient 0.97%	Corrected value
Direct: h=0	123 nH	(no correction) 123nH	0.97^0=1 (Not reflected)	123nH
2h=0.0030164	85.4 nH	(-2X) -171 nH	0.97^1	-165.676
4h=0.0060328	61.4nH	(+2X)+123	0.97^2	115.54252
6h=0.0090492	47.4nH	(-2X) -95	0.97^3	-86.5214004
8h=0.0120656	40.0nH	(+2X)+80	0.97^4	70.8234248
10h=0.0150820	31.1nH	(-2X)-62	0.97^5	-53.4132564
12h=0.0180984	25.9nH	(+2X)+52	0.97^6	43.14794986
14h=0.0211148	21.8nH	(-2X)-43	0.97^7	-35.22805203
16h=0.0241312	18.5nH	(+2X)+37	0.97^8	28.9985043
18h=0.0271476	15.8nH	(-2X)-32	0.97^9	-24.02330145
20h=0.030164	13.6nH	(+2X)+27	0.97^10	20.05793625
22h=0.0331804	11.8nH	(-2X)-24	0.97^11	-16.88111311
24h=0.0361968	10.2nH	(+2X)+20	0.97^12	14.15438416
26h=0.0392132	8.9nH	(-2X)-17	0.97^13	-11.9798822
28h=0.0422296	7.85nH	(+2X)+15	0.97^14	10.24952956
30h=0.0452460	6.91nH	(-2X)-14	0.97^15	-8.751531434
		20nH		23.5nH

The above table does not represent a converged set. The above table must be continued until the difference between Nh and (N+2)h are negligible, this occurs at about 50 pairs of reflections.

Even though the above table has not converged, we can deduce the general trend in the data. If we were to plot the greed data (97% reflectivity of copper) then the following chart is realized.

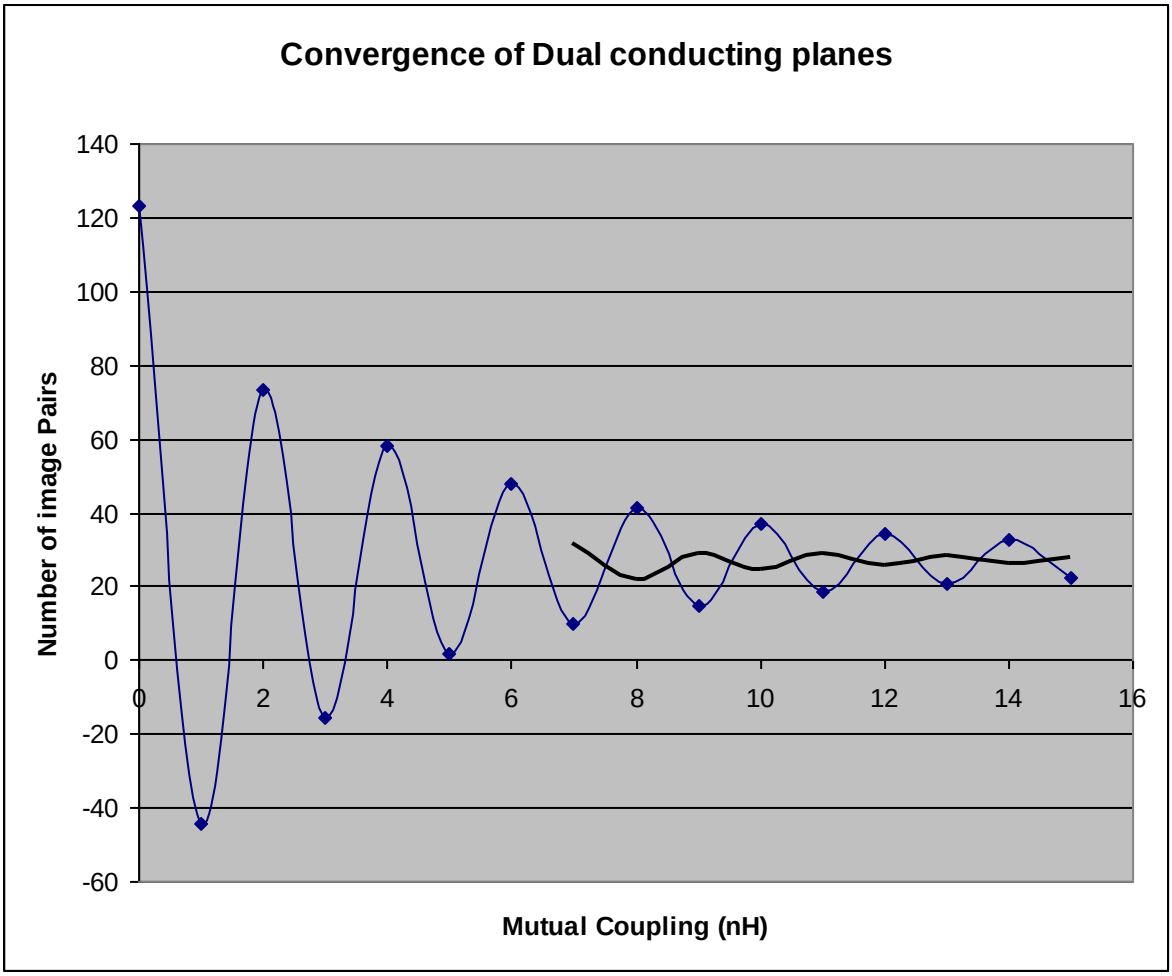

There are many way to find the converged value other than adding up 50 or more image pairs. A simple technique is disclosed here which is called "Guestimation"

With the "Guestimation" technique, the even values are plotted first, then a guess is made as to the true value of the mutual coupling. Then the odd points are plotted using the following expression: 2*(Guess value)-odd value. This results in the following plot for a guess of 25nH.

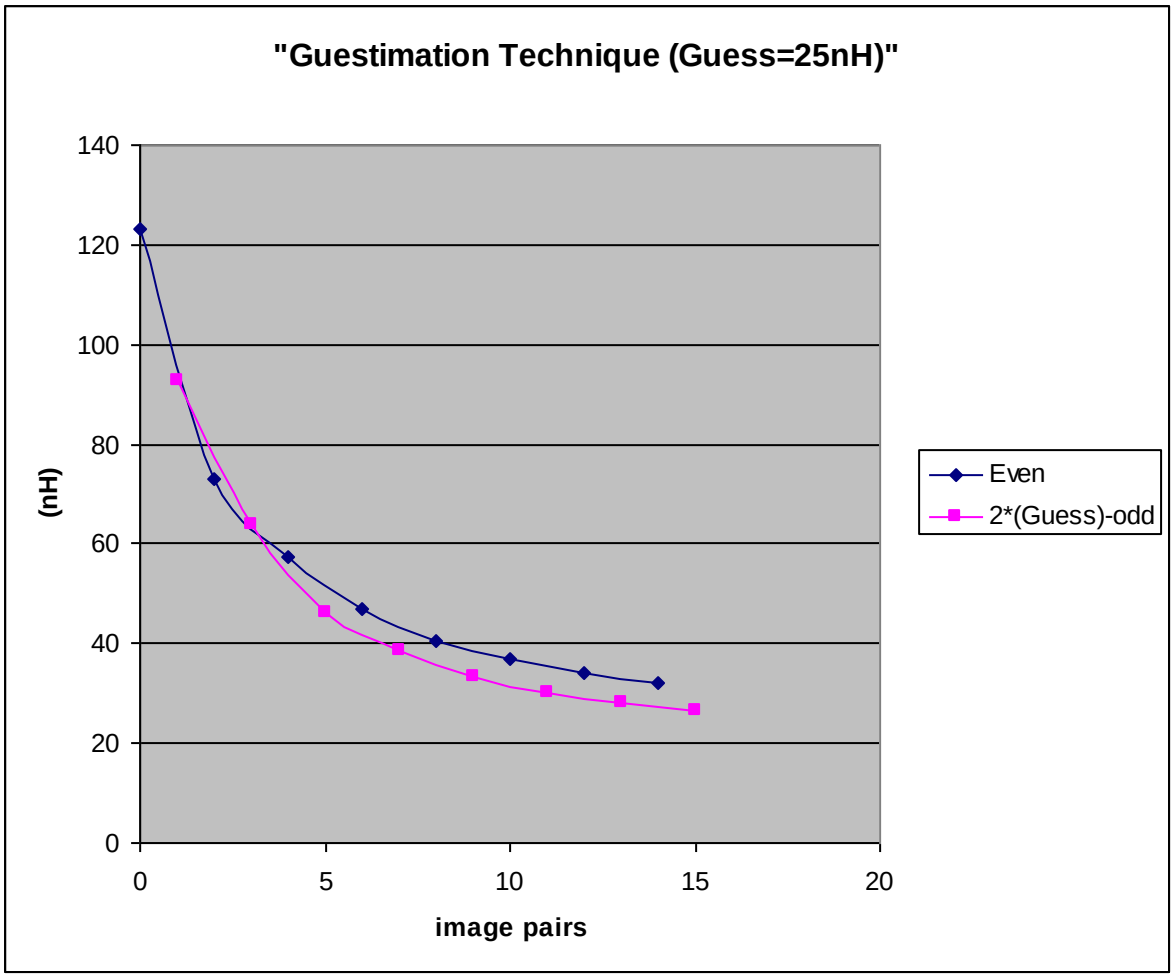

Then the guess is changed until there is good alignment in the plots as shown in the following diagram.

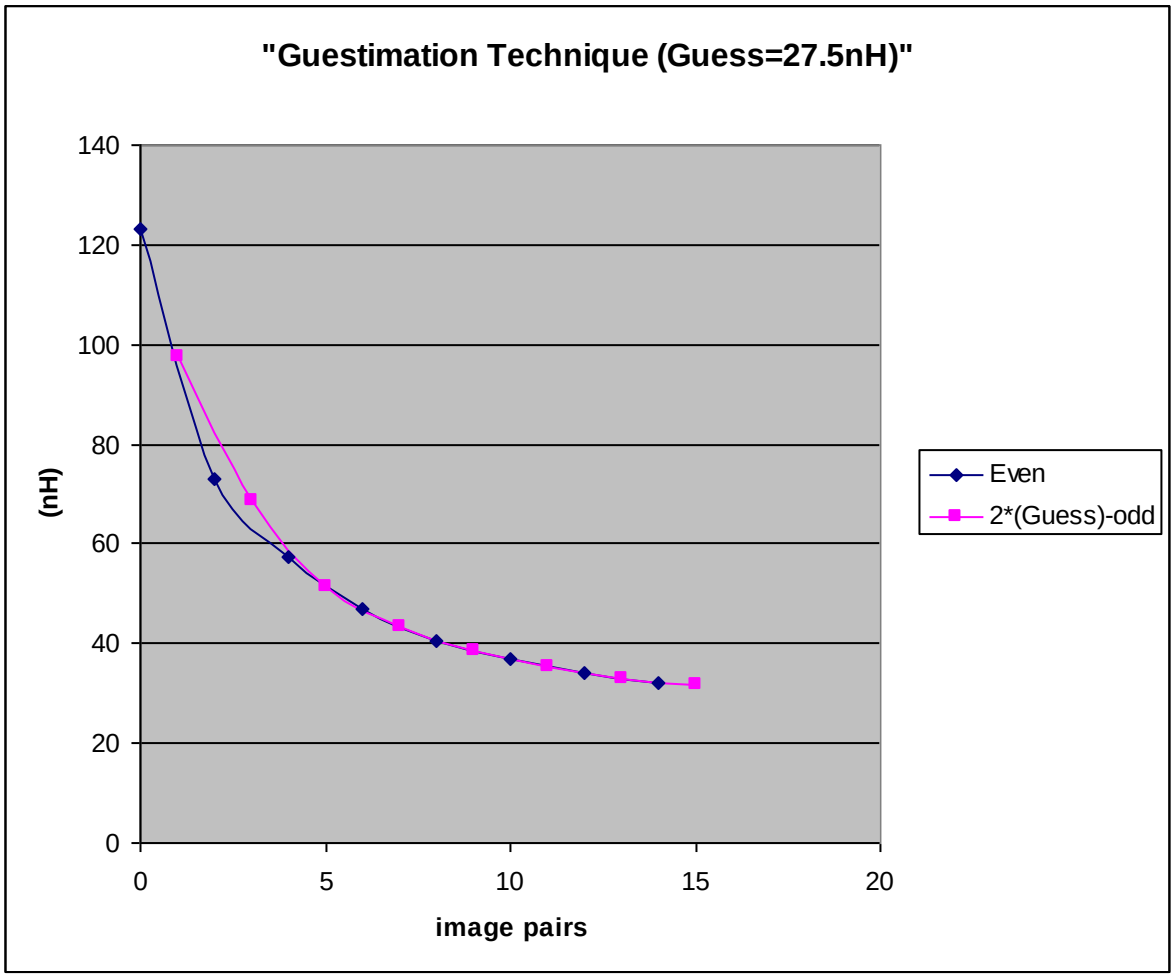

The above technique is done using an Excel spreadsheet.

The computed value of 27.5nH is in good agreement with the measured value of 27nH.

Note: The target loop is measured with a high impedance probe which only permits negligible current flow. If these experiments are conducted with a low impedance probe, the current developed in the target will provide another source of reflected energy that will affect the resultant coupling.

15.3.4 Coupling with outer parasitic loop

In this test, no conductive planes are used; instead, the outer square loop is closed with a jumper wire soldered across the pads. Because this loop is closed, it will permit induced currents to flow; which consequently, will affect the

coupling between the source and target (Secondary). The behavior of the outer loop is similar to parasitic arrays in antenna theory.

We have measured the resistance of the outer loop to be about 0.3 ohms. The inductance is measured to be 260nH which works out to an inductive reactance of 2*pi*6Mhz*260nH=9.8 ohms. Since 9.8 is much greater than 0.3, it is therefore possible to use the simplified relationship for parasitic reflection found in Equation 9-3.

The total coupling between source and target is then given by the modified relations ship:

$$M_{TOTAL} = M_{DIRECTT} - \frac{M_{OT}M_{SO}}{L_O}$$

The direct coupling is the same as determined in section 15.3.1. To calculate the mutual coupling between source and outer loop (M_{SO}), we use the Rectangular Loop Algorithm (section 8) with the following parameters:

Algorithm Parameter	Use
LX1,LY1	S=0.0508
LX2,LY2	Outer=0.05588 (2.2 Inches)
PX2,PY2	-2*d=-2*(0.00127)=-0.00254
PZ2	0
N1,N2	1
Result	98.0 nH

Next we determine the mutual coupling from the outer to the target (M_{OT}).

Algorithm Parameter	Use
LX1,LY1	outer=0.05588
LX2,LY2	T=0.05334
PX2,PY2	+d=0.00127
PZ2	0
N1,N2	1
Result	131 nH

Plugging in the above values and the measured value of 260nH for outer loop trace inductance yields

$$M = M_{DIRECT} - \frac{M_{OT}M_{SO}}{L_O} = 123 - \frac{98*131}{260} = 74.62nH$$

The measured value from Table 2, line 13 is 73.45nH.

There is excellent agreement between theory and experiment.

15.3.5 Trace Impedance reduction: Single Plane

As stated in section 14.1, the inductance of a trace can be reduced be the reflected coupling of itself from a conductive plane.

Note: this is not intended for evanescent transmission lines (such as microstrip). Follow-on work will cover high-frequency transmission lines and wave guides.

The total inductance of a trace is represented by the following

$L_{TOTAL} = L_C - \eta M_{REFLECTED}$.

The measured inductance of the outer loop (measured with no ground planes) is 260 nH.

Using the rectangular loops algorithm, we calculated the mutual inductance between the outer loop and its reflected image in the ground plane using the following parameters

Algorithm Parameter	Use
LX1,LY1	Outer=0.05588 (2.2 Inches)
LX2,LY2	Outer=0.05588 (2.2 Inches)
PX2,PY2	0
PZ2	2*0.0015082=0.0030164
N1,N2	1
Result	98.3 nH

Plugging the values into the relationship yields

L_{TOTAL} = 260nH – (0.97)98nH=165nH

The measured inductance of the outer loop with one ground plane is found in 15.2.3: Measured value = 169nH

There is excellent agreement between experimental and theoretical.

15.3.6 Trace Impedance reduction: Double Plane

This section considers the effect of two conductive planes on trace inductance (impedance).

Note: this is not intended for evanescent transmission lines (such as strip-line). Follow-on work will cover high-frequency transmission lines and wave guides.

Unlike section 15.3.3, where the mutual inductive coupling between the source and the target loops was drastically reduced by the addition of a second plane; the addition of a second plane for reducing trace impedance shows minimal change trace inductance as shown in the following experimental data (from section 15.2.3):

Outer loop trace inductance

- 260 nH with no conductive planes
- 169 nH with bottom conductive plane
- 153 nH with top and bottom plane

Parallel Conductive planes

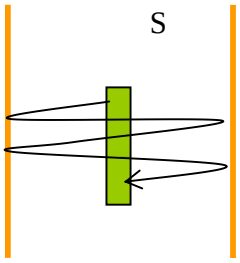

Figure 15-11: Parallel planes and inductance

As in the mutual induction example in section 10.2, there are reflected images of the source extending out to infinity (see Figure 10-3). The difference is that

the energy from each reflection must pass through the source. This causes another set of reflections as well as refractions. Since refractions are a topic of another book in the New Electromagnetism Application Series, we will not pursue it here. Needless to say, two conductive planes reduce the coupling between signal traces better than a single plane; however, not to the same degree as seen in the mutual case.

16 Conclusion

This book shows applications of the New Electromagnetic model for induction called New Induction. These applications are either difficult or impossible to model with classical electromagnetic theory.

The most amazing thing about this book is that all the couplings between circuits were derived, calculated and measured without once considering a field. The closest consideration of field theory was retarded time modeling where the propagation of the effects through space was considered. Beyond that, no time is wasted in calculating vector E or B fields.

The New Electromagnetic modeling of antennae provides a much more accurate result with much less work than the classical methods. New Electromagnetism requires only the consideration of the Inertial field for the far field derivation. The New Electromagnetic derivation shows that the longitudinal effects are paramount to deriving the proper radiation pattern. The longitudinal effects are not considered in classical theory since classical theory only describes a transverse magnetic field. This is the primary reason why antenna design was considered more "black magic" than science. Because the inductive field radiates spherically from a source, electromagnetic radiation is actually a spherical wave phenomenon which includes both transverse and longitudinal components.

The reflection of Inertial Fields from conductive surfaces is another topic that can not be derived from classical theory since classical theory requires a closed loop in order to derive the induced emf. The simple inductive MOI released in this paper enables the construction of new types of non-ferrous metal detectors that may have the ability to determine the type of metal detected.

There is much more New Electromagnetism research awaiting release.

Index

Antennae Modeling.....28
ARRL.....29
black magic.....28
Calculated Couplings.....**82**
Circuit to Measure Mutual Inductance.....48
coefficient of reflection.....60
Coupling with outer parasitic loop**87**
Coupling with single conductive plane.....**83**
Coupling with two conductive planes.....**84**
DC Mutual inductance.....12
Direct Coupling.....**82**
displacement current.....41
DVMx1000.....**81**
electromagnetic radiation..28, 41, 92
emf.....11
EMI.....**65**
Ethereal Mechanics.....41
Excel Algorithm.....22, 27, 45
half wave dipole.....28
inductance template.....**73**, **75**, **78**
Inductance template dimensions...**77**
inductance template measurments **81**
kinetic voltage 11, 32, 40, 48, 49, 53, 54, 55, 72
longitudinal wave.....28
Maxwell.....8, 28, 33, 41
Metal Detector.....56
Method of Images.....15
New Electromagnetic form of Kirchhoff's Law.....54
Parallel Conductive Planes.....59
Parallel Filaments.....22
Parallel Transverse Filaments.....17
Parasitic loops.....53
PCB / IC Trace Cross-Talk.....61
Perfect Earth model.....15
Position Sensing.....57
Q-Rise.....**61**
Rectangular Loop Example.....45
Rectangular Loops.....42
Reflected Coupling.....56
reflectometry.....**7**, **66**
refracted energy.....**65**
refractometry.....**66**
Relation between kinetic and potential voltages.....54
Retarded Time.....1, 13
Rules of Nature.....41
Self inductance.....13
Simple transistor current source....**78**
Simplified Reflected Coupling.....56
Single Conductive Plane.....58
spherical field.....41
spherical wave..... 28, 41, 92
Spherical Wave Model.....41
Stealth.....**66**
Trace Impedance reduction.....**89**
Trace Inductance of Outer Loop...**82**
Trace resistances.....**81**
Transformers.....**64**
transverse wave.....28
twin wire transmission system.....**70**
wire over ground plane transmission line.....**68**

